Light-Assisted Energy Storage Devices: Principles, Performance, and Perspectives

Dong, Ximan; Chen, Xinyue; Jiang , Xin & YANG, Nianjun (2023) Light-Assisted Energy Storage Devices: Principles, Performance, and Perspectives. In: Advanced Energy Materials, 13 (38) , p. 2301143.

DOI: 10.1002/aenm.202301143
Handle: http://hdl.handle.net/1942/40811

DOI: 10.1002/((please add manuscript number))
Article type: Review

Light-assisted energy storage devices: principles, performance, and perspectives

*Ximan Dong, Xinyue Chen, Xin Jiang, Nianjun Yang**

X. Dong, X. Chen, Prof. X. Jiang
Institute of Materials Engineering, University of Siegen, Paul-Bonatz Str. 9-11, Siegen, 57076, Germany

Prof. N. Yang
Department of Chemistry, Hasselt University, Agoralaan 1 – Buidling D, 3590 Diepenbeek, Belgium
IMO-IMOMEC, Hasselt University, Wetenschapspark 1, 3590 Diepenbeek, Belgium
E-mail: nianjun.yang@uhasselt.be

Keywords: energy storage; battery; supercapacitors; light-assisted devices

Abstract:

Various energy storage devices are highly demanded by our modern society. The use of solar energy, an important green energy source, is extremely attractive for future energy storage. Recently, photo-assisted energy storage devices have been rapidly developed since they efficiently convert and store solar energy, while their configurations are simple and their external energy decline is much reduced. Light-assisted energy storage devices thus provide a potential way to utilize sunlight at a large scale that is both affordable and limitless. Considering rapid development and emerging problems for photo-assisted energy storage devices, this review starts with the fundamentals of batteries and supercapacitors and follows with the state-of-art photo-assisted energy storage devices where device components, working principles, types and practical applications are explained. After the detailed demonstration of some photo-assisted energy storage devices examples, the bottleneck of such light-assisted energy storage

devices is discussed and the prospects of the light-assisted rechargeable devices are further outlined.

1. Introduction

Global energy consumption daily increases with the dramatic development of industry, while the available amount of fossil fuels is significantly reduced. However, technological and economic development needs the increased combustion of fossil fuels, which leads to dwindling storage, environmental pollution, and extreme weather.[1,2] In order to fundamentally solve the problems of both energy depletion and environmental pollution, the search and development of clean and renewable energy sources have been becoming the research spotlight worldwide. As a green, renewable and buckshee source, solar energy possesses unlimited prospects for its application.[3] More and more forms of solar energy have been thus recently utilized. With aid of numerous photovoltaic (PV) devices and electronic equipment, solar radiation energy is photoelectrochemically converted into electrical energy. Such an integrated technique is one of the important forms of solar energy utilization.[4–6]

It is well-known that a solar cell can convert solar energy into electrical energy, but the energy cannot be continuously stored. To overcome such a challenge or to achieve efficient use of solar energy, different solar PV systems have been combined with other electrochemical energy storage devices such as supercapacitors (SCs) and batteries.[7] Among various energy devices, rechargeable batteries such as lead-acid batteries and Li-metal batteries have been proven to be the most effective for such integrated energy storage systems.[8] This is because rechargeable batteries utilize the mutual conversion between electrical energy and chemical energy to achieve energy conversion and storage. They have been even widely used in electric vehicles, mobile/portable electronic devices, and many other fields. Once solar energy is harvested and further storage inside rechargeable batteries, large-scale utilization of solar energy is expected. Meanwhile, such photo-induced energy storage devices are helpful to reduce the input and/or increase the output powers of conventional rechargeable batteries.

Since last century, significant progress and achievements have been obtained in both rechargeable batteries and solar cells. However, the integration of different rechargeable batteries with PV cells still remains a great challenge, especially in the aspects of producing efficient and cost-effective energy storage devices. In other words, how to achieve effective, more economic, durable and environmentally friendly integration of solar energy into different rechargeable batteries is challenging. It has been revealed that the storage of solar energy inside rechargeable batteries generally involves two processes: the conversion of solar energy to electrical energy in the solar cell and the conversion of electrical energy to chemical energy in the batteries.[9–11]

Since the first photo-rechargeable battery was developed by Hodes and colleagues in 1976,[12] various photo-assisted energy storage devices have been designed, developed, and produced. Note that early solar rechargeable batteries typically utilized separated cells to store the electrical energy that was generated from solar energy *via* an external circuit.[13] Unfortunately, such external combinations often involved complex device architectures, additional PV conversion modules, and external components. Namely, they led to energy losses and reduced energy conversion/storage efficiencies. Meanwhile, they featured increased operating costs and added weights/sizes of the devices. For feasible solar energy conversion and storage, a two-electrode photo-enhanced battery was reported in 2002 for the first time.[14] In this solar cell a dye-sensitized photoactive layer was used for the photoelectric conversion and iodine ion-electron pairs (I^-/I_3^-) were for the charging/discharging steps. Later in 2004, the first two-electrode light-driven capacitor was proposed, where a dye-sensitized nanocrystalline film was incorporated with two layers of active carbon particles.[15] Later on, the direct integration of PV cells with various energy storage devices (e.g., SCs, rechargeable batteries) continuous increasing. From the historic timeline of the development of these photo-assisted energy storage devices (**Figure 1**),[12,14–23] one can divide these devices into two- or three-electrode systems or configurations. It must highlight here that SCs and rechargeable metal batteries have emerged as the best options for the construction of various photo-enhanced energy storage devices, where utilization efficiencies of solar energy have been improved. Namely, solar energy can be directly stored during the charging processes of various photo-assisted rechargeable batteries.

It is also effective for enhanced discharge performance in certain devices through a so-called photoelectric effect. On the other side, the fabrication of better photo-responsive energy storage devices remains challenging, especially those with higher performance (e.g., energy conversion efficiencies), more compacted structures, and better compatibility of the solar cells with the batteries.[24,25]

It is worth mentioning that such solar-driven energy storage devices are popular and critical for recently and rapidly developed wearable devices and flexible electronics. In these cases, the design of miniature and portable flexible energy storage devices is extremely important.[26,27] The high-power consumption of multiple components inevitably leads to inconvenience in terms of early battery replacement or the applications of frequent charging processes. If a flexible energy storage device with a high-volume energy density is integrated into a wearable device that needs to be frequently subjected to repeated mechanical stress, the safety issue arises.[28,29] In this context, a light-assisted charging system is quite promising in that it can directly absorb sunlight and further convert solar energy into electricity. An external power source is thus not necessary or required. This review article summarizes the state-of-art of photo-enhanced/driven/assisted/induced energy storage devices. It starts from a brief description of the various components of such devices and continues with the principles of charging/discharging photo-enhanced energy storage devices. This section specifically summary and analyzed the charge transfer between electrode materials and variations in electrochemical properties (like CVs and GCD curves) after the intervention of light. The progress and achievements of photo-enhanced energy storage devices are then presented and detailed in terms of their device components and performance evaluation. In particular, this review provides a separate summary of developing some recent flexible light-assisted devices as well as all-solid-state devices. In the last part of this review, the challenges and opportunities of such light-enhanced energy storage devices are discussed and outlined.

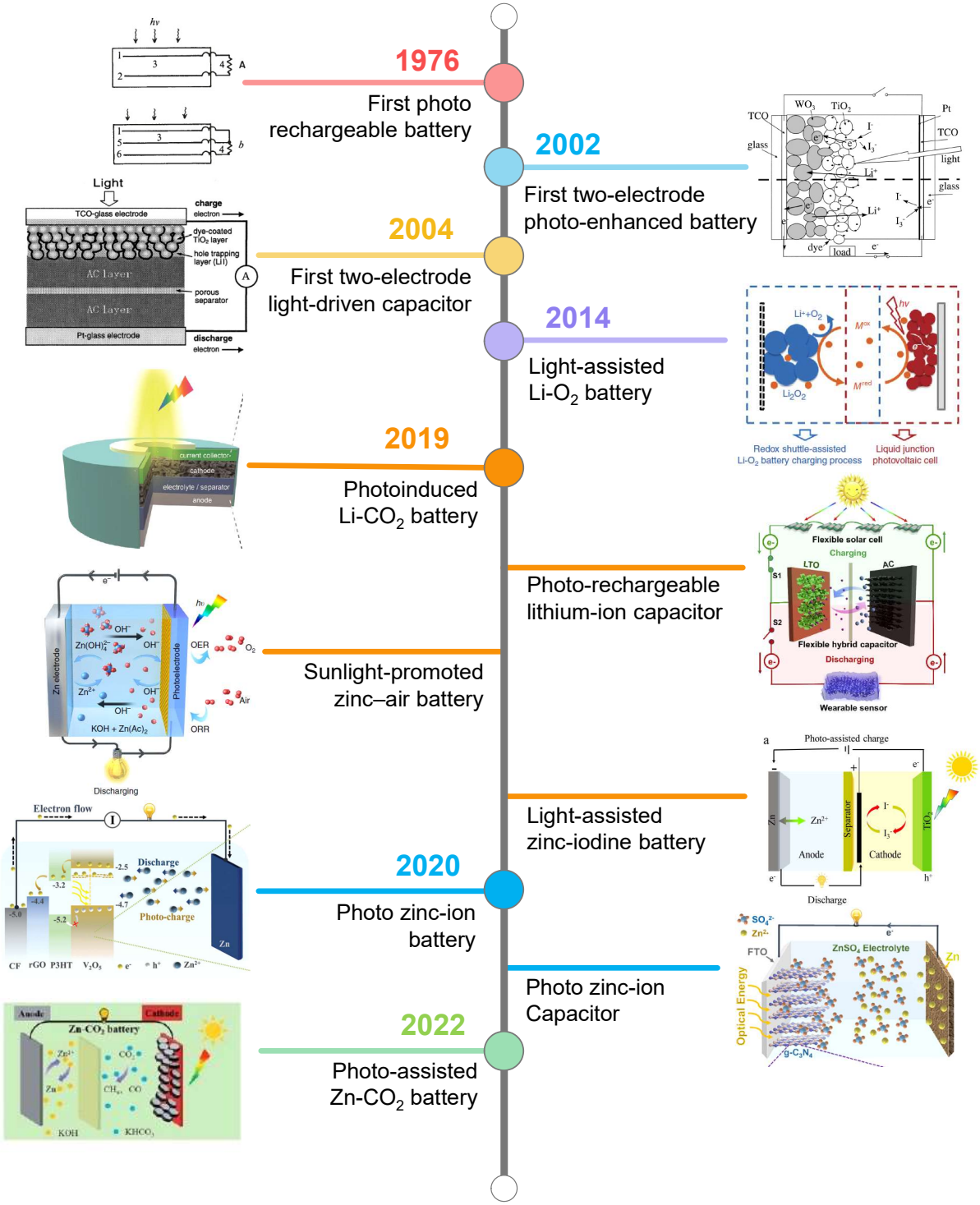

Figure 1. The development timeline of photo-assisted energy storage devices. Reproduced with permission.[12,14–23] Copyright 1976, 2014, 2019, Springer Nature. Copyright 2002, The Electrochemical Society. Copyright 2004, American Institute of Physics. Copyright, 2019, 2020, Elsevier. Copyright, 2019, 2020, Wiley-VCH. Copyright, 2020, 2021, Royal Society of Chemistry.

2. Working principles of photo-assisted energy storage devices

A photo-assisted rechargeable energy storage device holds multiple roles or functions: solar energy harvesting, conversion, and storage. Such a device thus consists of two parts: one part is responsible for the collection and conversion of sunlight.[30] Another part is responsible for energy storage. Among energy storage devices, electrochemical ones, namely different batteries and SCs have been extensively developed, including those equipped with solar cells. At an early stage, these devices were simply assembled by connecting two devices with a metal wire. Therefore, those are not truly photo-assisted devices. In recent years photosensitive or semiconductor materials have been gradually added to these energy storage devices or compounded with electrode active materials to form different photoelectrodes. In these single devices, the conversion and storage of solar energy have been achieved. After the engagement of light, an energy storage device can harness the power of light energy to facilitate its fast charging and its enhanced energy density. Some light-assisted devices can even possess the ability of self-charging under ambient light illumination, eliminating the need of external electrical charging. This feature is particularly useful in low-power applications and for remote areas where access to conventional charging methods is much limited. Particularly, the introduction of light into metal batteries not only accelerates the reaction kinetics of the cell, but also optimizes the performance of the applied catalyst.[31,32] For example, the utilization of photoelectrochemical processes facilitated or accelerated different reactions (e.g., oxygen reduction reaction, oxygen evolution reaction), eventually leading to improved reaction kinetics, increased efficiencies, and enhanced overall battery performance. Prior to presenting the details of these photo-assisted energy storage devices, the working principles of two standard electrochemical energy devices – SC and battery are briefly introduced, followed by the device components of photo-assisted energy storage devices.

2.1 Supercapacitor concept

The supercapacitor is an energy storage device, which structural composition is similar to a battery. It consists of a positive electrode and a negative electrode that is immersed in an electrolyte. Two electrodes are separated by an ion-permeable electron-insulating film. During

its energy storage process, the adsorption/desorption of ions or electrochemical reactions occur at the (porous) electrode surface. Namely, the charge transfer undergoes at the interface between the (porous) electrode or an electrochemically active material and the electrolyte.[33]

Depending on their energy storage mechanisms, SCs can be divided into electrical double-layer capacitors (EDLCs) and pseudocapacitors (PCs). An EDLC (**Figure 2a**) is an electrochemical capacitor that stores electrostatic charges by reversible adsorption/desorption of electrolyte ions on the electrode surface.[34] There is no Faraday chemical reaction during the charge storage process, which is a physical process. The energy is stored in the electric field created between the charged electrode and the electrolyte. The EDLCs predominantly employ carbon-based materials (e.g., activated carbon, carbon nanotubes (CNTs), graphene, and carbon aerogels). These materials have high surface areas and provide an ideal platform for the adsorption of ions, enabling the formation of large electric double layers.[35] Since an EDLC mainly uses electrostatic adsorption/desorption of charges or electrons to store energy, the involved charges during the charging/discharging process are the same, which can be calculated by integrating related cyclic voltammograms (CVs, **Figure 2b**). More exactly, the anions and cations in the electrolyte move directionally toward the electrodes under constant potential conditions during a charging step, leading to the adsorption or accumulation of positive and negative charges on each side of the electrodes, namely the formation of electric double layers on both electrodes. During a discharging step, the charges are desorbed or released from both electrodes. In the course of such a charging/discharging process, no (electro)chemical reactions occur on the electrode(s) or in the solution. The concentrations of ions in the electrolyte remain constant, contributing to the excellent cycling performance of an EDLC. Theoretically, the times for the charging and discharging processes of an EDLC are the same. The galvanostatic charge-discharge (GCD) curves of an EDLC during the charging/discharging process are triangle shape and mirror-like, even at different current densities. However, the involvement of equivalent series resistances (ESRs) of both electrodes leads to the decay of storing and releasing related charges (**Figure 2c**). Different from an EDLC, the performance of a PC is relied on highly reversible adsorption/desorption reactions or Faraday redox reactions at the electrode surface, which are the source of energy storage of a PC.[36] These reversible chemisorption/-desorption

processes occur not only at the electrode surface but also deeply into the bulk of the electrode material **(Figure 2d)**. The redox reaction is influenced by the factors such as the specific surface area, composition, valence state change, and structure of the electrode material. To construct a PC, the commonly used materials include metal oxides and hydroxides (e.g., RuO_2, MnO_2, TiO_2, Fe_3O_4, $Ni(OH)_2$, Co_3O_4),[37–41] and conducting polymers (e.g., poly(3,4-ethylenedioxythiophene)/polystyrene sulfonate: PEDOT/PSS, polypyrrole: PPy and polyaniline: PANI)[42–45]. These active materials possess many electroactive sites that can undergo reversible redox reactions by donating or accepting electrons. In most cases, the specific capacity and energy density of a PC are thus generally higher than those of an EDLC. Meanwhile, a PC works similarly to a battery in that it stores and releases charges on the base of Faraday redox reactions. Sometimes a PC is also named as a Faraday capacitor. Note that a Faraday capacitor refers more to a PC, where occurs underpotential deposition (UPD) of electrochemically active materials on the surface of an electrode or on the two-dimensional/quasi-two-dimensional spaces within the bulk phase. In the charging step of a PC, the charges are stored through both highly reversible adsorption/desorption of ions and fast redox reactions where anodic peaks appear in some cases (**Figure 2e**). These stored charges are released during the discharge step, leading to the appearance of cathodic peaks in most cases. In the GCD curves of a PC (**Figure 2f**), the plateaus are often seen together with linear ranges that belong to an EDLC.

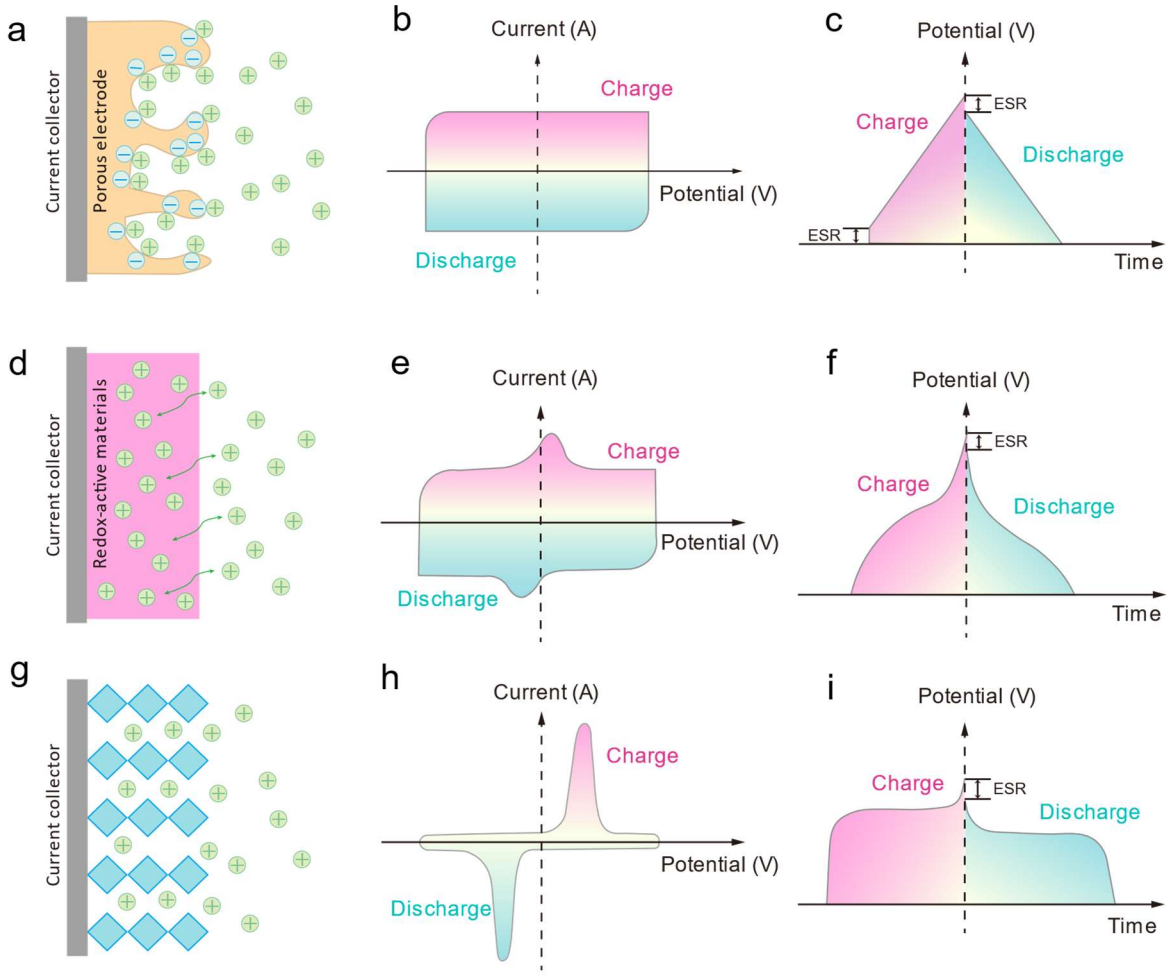

Figure 2. The working principles, CVs, and GCD curves of (a-c) an EDLC, (d-f) a PC, and (g-i) a battery.

2.2 Battery concept

Batteries can be generally divided into the disposal and rechargeable ones. A battery typically consists of two electrodes: an anode and a cathode. They are separated by an electrolyte. The energy storage process in a battery no longer relies on physical adsorption to store charge, as that occurs in an SC. It relies predominantly on reversible electrochemical reactions involving metal ions, such as Li^+, Zn^{2+} or Na^+ **(Figure 2g)**. Taking a LIB as an example, Li ions are reduced to lithium metal during the charging process, while lithium metal reversibly oxidized into lithium ions during the discharge process. During the charging process, a battery is connected to an external power source, which causes an electrical current to the battery. These current drives a reversible electrochemical reaction within the battery, converting the chemical energy stored in the anode and cathode into electrical energy that can be stored in a battery.

When a battery is discharged, the stored electrical energy is converted back into chemical energy when the electrochemical reaction is reversed. The reversible intercalation of metal cations shows prominent peaks in the CV of a battery **(Figure 2h)** and the plateaus in its GCD curve **(Figure 2i)**, which are associated with the reduction and oxidation of the metal centers involved in the charge storage/release processes.

Among various types of rechargeable batteries, lithium-ion secondary batteries have been widely studied in recent years and further employed as the power suppliers of portable electronic devices, stemming from their cleanness, high efficiencies/capacity, and lightweight.[46] Meanwhile, their drawbacks are quite obvious: high prices, due to the limited and unevenly distributed lithium resources. In these regards, the construction and development of secondary batteries using other alkali metal ion batteries such as sodium and potassium ion batteries have been attracting extreme attention in the so-called post-lithium battery decade.[47] This is because sodium and potassium are more abundant in the earth's crust and thus much cheaper than lithium. More importantly, their electrochemical properties are similar to lithium. In addition to sodium and potassium ion batteries, zinc-ion batteries have received lots of attention, owing to their higher safety and lower cost than other batteries.[48]

2.3 Light-assisted energy storage concept

Nowadays, the integration of both of SCs and batteries, especially relatively mature developed lithium-ion batteries and relatively safe zinc-ion batteries with different PV devices gives birth to new light-driven energy storage devices. **Table 1** shows the configurations of representative light-assisted energy storage devices based on various cells and photocathodes. In some reports, they have been also named as light-induced energy storage devices. In this article, we adopt light-assisted energy storage devices throughout the whole text.

Table 1: Configurations and performance of representative light-assisted energy storage devices.

Type	Photo electrode	Light source	Current density	Capacitance or capacity	Energy density (mWh cm^{-2})	Solar conversion (SC) or photo enhancement (PE) efficiency	Cycle or Lifetime (h)	Ref
Supercapacitor	Fe_2O_3@$Ni(OH)_2$	100 mW cm^{-2}	0.1 mA cm^{-2}	20.6 mF cm^{-2}			66% (1000 cycles)	64
	$CH_3NH_3PbI_3$	100 mW cm^{-2}		2.35 mF cm^{-2}		25% (SC)		56
	CF@CuO_x@$NiCuO_x$	1.76 W	5 mA cm^{-2}	2.64 F cm^{-2}		44%	80.16% (1500 cycles)	63
	Carbon dots modified $Ti_3C_2T_x$	PLS-LED 100 150 mW·cm^{-2}	10 A cm^{-3}	1445 F cm^{-3}	18.75 mWh·cm^{-3}	35.9%	8000 cycles	150
Hybrid	2D g-C_3N_4	50 mW cm^{-2}	5 mA g^{-1}	11377 mF g^{-1}	668 mWh kg^{-1}	82%	~90% (1000 cycles)	20
capacitor	Ag@V_2O_5	12 mW cm^{-2}	1000 mA g^{-1}	138 F g^{-1}	53 Wh kg^{-1}	63%	~99% (4000 cycles)	65
	ITO/PET	AM 1.5 G	1 A g^{-1}		40 Wh kg^{-1}	8.41% (SC)	85% (2000 cycles)	17
Li-ion battery	TiO_2/dye/Cu_2S	Xe lamp	100 mA g^{-1}	209 mAh g^{-1}			71% (10 cycles)	78
	V_2O_5/P_3HT/rGO	12 mW cm^{-2}	1 mV s^{-1}	161 mAh g^{-1}		57%	175 cycles	79
	organic molecule (TKL)	405 nm violet laser	50 mA g^{-1}	332 mAh g^{-1}		12%		80
Li-O_2 battery	TiO_2–Fe_2O_3	500 W Xe lamp	0.01 mA cm^{-2}				86% (100 cycles)	88
	WSe_2	lab Xenon	0.15 mA cm^{-2}	33.03 mWh cm^{-2}		270%	120h	122
Li-CO_2 battery	SiC/RGO	500 W Xe-lamp	20 mA g^{-1}	4996 mAh g^{-1}		212%	80 cycles (100 mA g^{-1})	89
	CNT@C_3N_4	350 W Xenon lamp	0.1 mA cm^{-2}	15.77 mAh cm^{-2}			86.1% (100 cycles, 0.01 mA cm^{-2})	90
	In_2S_3@CNT/SS		0.01 mA cm^{-2}			15%	50h	22
Li-I_2 battery	I_2@AC/N719-dye/TiO_2	2000 lm LED white light	100 mA g^{-1}	193 mAh g^{-1}		16.2%	80% (100 mAh g^{-1})	94
Li-S battery	CdS-TiO_2/carbon cloth	500 W Xe lamp		1225 mAh g^{-1}		10%		98
	TiO_2	300W Xe lamp	500 mA g^{-1}	885 mAh g^{-1}		38%	47.7% (50 cycles)	99
Zn-ion battery	rGO/P_3HT/V_2O_5/Ag	12 mW cm^{-2}	50 mA g^{-1}	370 mAh g^{-1}		95%	~75% (500 cycles 500 mA g^{-1}, dark)	21
	FTO/ZnO/VO_2/Ag	12 mW cm^{-2}	200 mA g^{-1}	432 mAh g^{-1}		17.7%	73% (500 cycles, 1000 mA g^{-1}, dark)	101
	CF/rGO/VO_2	12 mW cm^{-2}	200 mA g^{-1}	315 mAh g^{-1}		11.7%	79% (250 cycles, 5000 mA g^{-1})	102
	FTO/ZnO/MoS_2/Ag	12 mW cm^{-2}	100 mA g^{-1}	340 mAh g^{-1}		38.8%	~82% (200 cycles, 500 mA g^{-1}, dark)	103
	Co_2P-CoPNiCoO_2	68.5 mW cm^{-2}	2 A g^{-1}		366 Wh kg^{-1}	6.4%	78% (25000 cycles, 32 A g^{-1})	104
Zn-O_2 battery	composite (α+δ)-MnO_2	150 W visible light lamp		715 mAh g^{-1}	841.55 Wh kg^{-1}	7.20%		151
	pTTh/CP	100 mW cm^{-2}				29.0%	64h (0.1 mA cm^{-2})	110
	PDTB/TiO_2 CP	90 mW cm^{-2}					22h (5 mA cm^{-2})	111
Flow battery	dual-silicon	AM 1.5-G		730 mAh L^{-1}		3.2% (SC)	37h	114
	α-Fe_2O_3/PANI	100 mW·cm^{-2}				0.08% (SC)		115
	silicon-based	100 mW cm^{-2}		2.27 Ah L^{-1}	1.52 Wh L^{-1}	5.4% (SC)	80% (200h, 5 mA cm^{-2})	117

2.3.1 Working principles

A light-assisted energy storage device consists of a photocathode (light-absorbing material and electrode active material) and an anode. During its photo-charging process, both the photocathode and the anode are connected to an external circuit. Under light illumination, the light-absorbing material (e.g., a semiconductor) receives the photons, leaping the electrons (e^-) in the valence band to the conduction band of the semiconductor. A positively charged hole (h^+) is then generated in the valence band, producing an electron/hole pair (Eq. 1).

$$hv \rightarrow \text{photocatalyst} \rightarrow h^+ + e^- \quad (1)$$

When the photogenerated holes of light-absorbing material diffuse to the electrode active material surface, an oxidation reaction undergoes on the cathode, namely C^R to C^o (Eq. 2):

$$C^{\mathrm{R}} + h^+ \rightarrow C^{\mathrm{O}} \quad (2)$$

Meanwhile, the photogenerated electrons in the conduction band can transfer to the anode *via* the external circuit. **(Figure 3a)** They can be injected into the anode and thus a reduction reaction happens on the anode, namely A^o to A^R (Eq. 3).

$$\mathrm{A^O} + \mathrm{e^-} \rightarrow \mathrm{A^R}\ (\textit{via}\ \text{circuit}) \quad (3)$$

In this way, the potential difference between a redox pair of the positive and negative electrodes can be used to calculate discharge energy of a solar-driven device. In this device, the ion transport flows through the diaphragm to balance the internal charge. During this photo charging process, the energetic potential (E_c) of the C^O/C^R pair is positive, while that (E_a) of the A^O/A^R pair is negative. They correspond to the harvested solar energy that is electrochemically stored.

During the discharging process of a solar-driven device, the cathode and anode are connected to an external load. Electrons flow from the anode to the cathode, resulting in the reduction of the active material(s) on the cathode side (Eq. 4) and meanwhile the oxidization of the active material(s) on the anode side (Eq. 5)**:**

$$C^{\mathrm{O}} + \mathrm{e^-} \rightarrow C^{\mathrm{R}} \quad (4)$$

$$A^{\mathrm{R}} \rightarrow A^{\mathrm{O}} + e^- \quad (5)$$

During the discharging process, the device converts the stored chemical energy into electrical energy. Thermodynamically speaking, the discharging process is reversed to a charging one.

For different energy storage systems there are different operating principles and specific reaction equations (Table 2), where the cathodes are as the light electrodes and M as photosensitive or semiconductor materials.

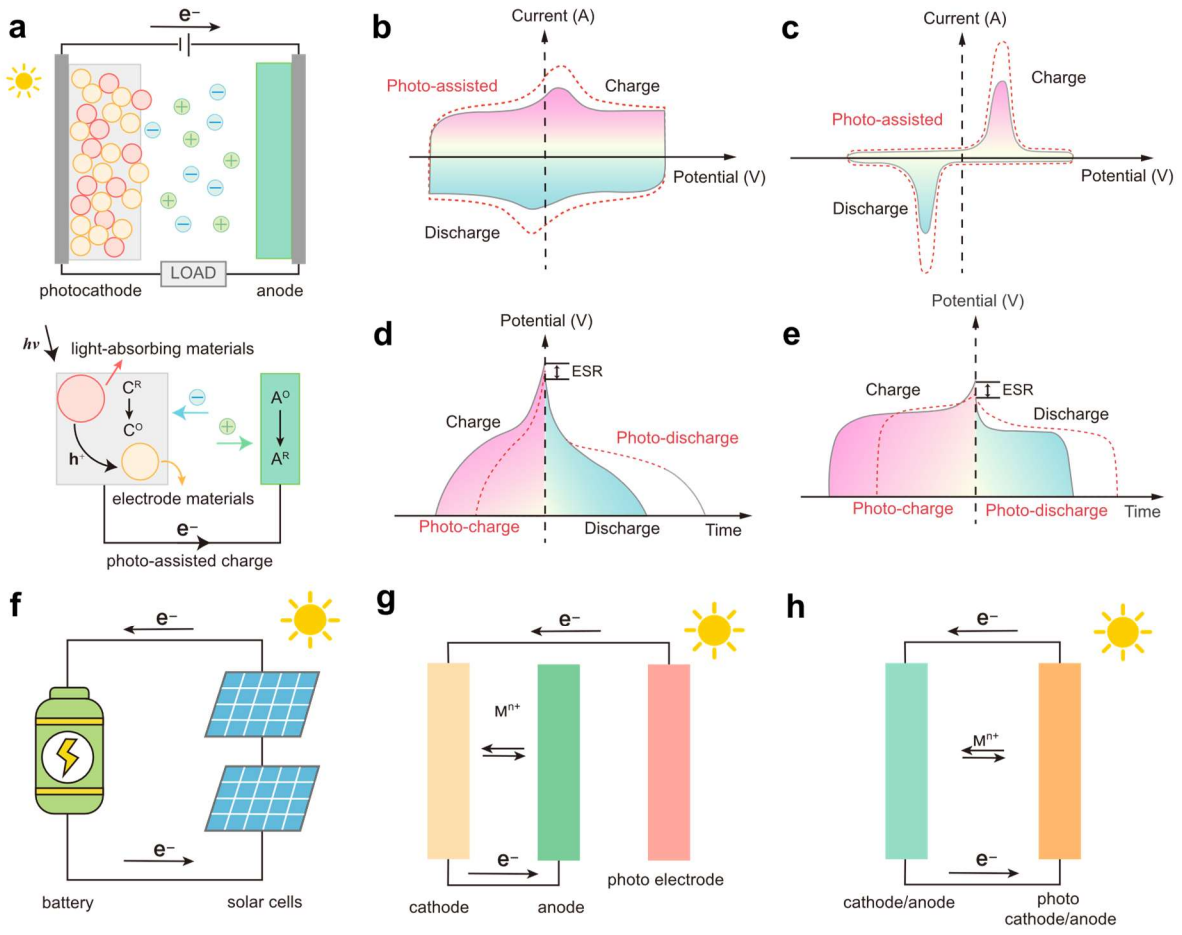

Figure 3. (a) Working principle of a photo-assisted energy storage device; The CVs and GCD curves of (b,c) a photo-assisted SC and (d,e) a photo-assisted SC battery; The classification of photo-induced energy storage devices: a PV cell is connected with a storage device. (f) They individually work as two separate devices, (g) a three-electrodes device, (h) a two-electrode device.

The CVs and GCD curves of a photo-assisted SC and battery are schematically illustrated in **Figure 3b** to **Figure 3e**. In the CVs of a photo-assisted SC (**Figure 3b**) and a photo-assisted SC battery (**Figure 3c**), it is clear that the photogenerated charges synergistically accelerate electron transfer and ion diffusion kinetics, which leads to aggrandizement in currents,

especially anodic and cathodic peak currents. In the GCD curves of a photo-assisted SC (**Figure 3d**) and a photo-assisted SC battery (**Figure 3e**), the introduction of light into a charging process speeds up the charging rate and shortens the charging time, while the discharge rate slows down during the discharging process. Light-assisted devices have the potential to achieve higher energy densities or more efficient energy storage. This is because they can provide greater energy capacity in smaller and lighter devices. Meanwhile, the performance, stability and lifetime of light-assisted devices is expected to be improved compared to non-light-assisted devices with aid of the optimized light-based energy conversion mechanisms. This is particularly for some metal-air cells that have high overpotentials. Light intervention can then effectively improve the stability of the device, and eventually enhance the capacity and cycling life of such a light-driven device.

Table 2: Working mechanisms of representative light-assisted batteries.

		Discharge	Charge	Overall
Li-ion battery	Anode	$Li \rightarrow Li^+ + e^-$	$Li^+ + e^-(M) \rightarrow Li$	$Li_xM_y \leftrightarrow Li^+ + Li_{(x-1)}M_y$
	Cathode	$Li^+ + e^- + Li_{(x-1)}M_y \rightarrow Li_xM_y$	$Li_xM_y + h^+(M) \rightarrow Li^+ + M + Li_{(x-1)}M_y$	
Li-O_2 battery	Anode	$Li \rightarrow Li^+ + e^-$	$Li^+ + e^- \rightarrow Li$	$Li_2O_2 + 2Li^+ \leftrightarrow O_2 + 2Li$
	Cathode	$O_2 + 2e^- + 2Li \rightarrow Li_2O_2$	$Li_2O_2 + 2h^+(M) \rightarrow O_2 + 2Li$	
Li-CO_2 battery	Anode	$Li \rightarrow Li^+ + e^-$	$Li^+ + e^-(M) \rightarrow Li$	$2Li_2CO_3 + C \leftrightarrow 4Li + 3CO_2$
	Cathode	$4Li^+ + 3CO_2 + 4e^- \rightarrow Li_2CO_3 + C$	$Li_2CO_3 + C + 4h^+(M) \rightarrow 4Li^+ + 3CO_2$	
Li-I_2 battery	Anode	$Li \rightarrow Li^+ + e^-$	$Li^+ + e^-(M) \rightarrow Li$	$3I^- + 2Li^+ \leftrightarrow I_3^- + 2Li$
	Cathode	$I_3^- + 2e^- \rightarrow 3I^-$	$3I^- + 2h^+(M) \rightarrow I_3^-$	
Zn-ion battery	Anode	$Zn \rightarrow Zn^{2+} + 2e^-$	$Zn^{2+} + 2e^-(M) \rightarrow Zn$	$Zn_xM_y \leftrightarrow Zn^{2+} + Zn_{(x-1)}M_y$
	Cathode	$Zn^{2+} + 2e^- + Zn_{(x-1)}M_y \rightarrow Zn_xM_y$	$Zn_xM_y + 2h^+(M) \rightarrow Zn^{2+} + Zn_{(x-1)}M_y$	
Zn-O_2 battery	Anode	$Zn + 4OH^- \rightarrow 2e^- + Zn(OH)_4^{2-}$	$Zn(OH)_4^{2-} + 2e^-(M) \rightarrow Zn + 4OH^-$	$2ZnO \leftrightarrow 2Zn + O_2$
		$Zn(OH)_4^{2-} \rightarrow ZnO + H_2O + OH^-$		
	Cathode	$O_2 + 4e^- + 2H_2O \rightarrow 4OH^-$	$4OH^- + 4h^+(M) \rightarrow O_2 + 2H_2O$	

When light-assisted energy storage devices undergo photoelectric conversion, they inevitably generate thermal effects, which are often overlooked. In some cases, the absorption of light by a battery or its components can lead to localized heating. Excessive heat can negatively impact battery performance and shorten its lifespan. Although there are some disadvantages, some benefits exist. For example, the electrode material absorbs photons and generates heat, resulting in a lower interfacial transport resistance, eventually accelerated reaction kinetics and variable

operating conditions.[49] Therefore, the management of the photothermal effect is crucial to prevent overheating these batteries and to further maintain their efficiencies. Such a device was thus stable at extremely low temperatures, due to the self-heating feature of the battery.[50,51] Further research of synergistic photovoltaic and photothermal conversion of a solar cell is expected to lead to breakthroughs and development of light-assisted energy storage technology with higher performance.

2.3.2 Device components and classification

Several integration/combination strategies have been developed for the direct conversion and/or storage of solar energy in PV cells. Specific parameters or technical indicators are believed to be indicative for different electrode systems that used for light-assisted energy storge devices. In this review article, the construction type is employed as the parameter to determine different working principles and applications of these light-assisted devices. Namely, three main combinations exist: a conventional solar cell/energy storage hybrid device, a light-assisted three-electrode device configuration, and a two-electrode device configuration. The conventional solar cell/energy storage hybrid devices are generally large, inflexible, costly, and energy-losing.[25,52] In contrast to energy storage devices or solar cells, light-assisted devices have photosensitive or semiconductor materials in the electrodes that produce holes and electrons in the presence of light, converting sunlight into electricity suitable only for immediate use or grid injection and enabling self-charging. The relevant principles have been described in previous sessions. They combine the functions of energy capture and storage in a single device. Therefore, they convert light energy directly into chemical energy, allowing energy to be captured and stored simultaneously. This eliminates the need to separate energy storage systems and increases overall energy efficiencies of such devices. Moreover, light-assisted energy storage devices can offer high charge and discharge rates, enabling rapid energy storage and release. This feature makes them suitable for the applications that require quick bursts of energy or where intermittent energy availability is a concern. Note that light-assisted energy storage devices are still under development and not yet as mature. Few of them are commercially

prevalent as traditional solar cells. However, they hold promise for future energy storage applications, again in that they combine energy capture and storage in a single device, offering increased efficiencies, versatility, and potential integration options. To achieve a high-efficiency of PV cell, the internal integration of the photo response function into a cell with a two-electrode configuration is certainly a potential solution and thus has recently attracted increasing attention. The integrated two-electrode cells feature excellent photo response capability. They directly convert/store captured solar energy and alleviate the energy density problems of the PV cells. The types of connections of these devices and their working principles are described in the following section.

Type I: Solar cell/energy storage hybrid devices

In hybrid devices, a PV cell and a storage device are individually connected as two separate devices by use of an external circuit **(Figure 3f)**. Consequently, each part is an integral part and can independently operate. The solar part or the PV cell is responsible for the conversion of solar energy into electricity as well as the subsequent storage of harvested energy through an external circuit in the energy storage device. Since the development of both independent devices is mature, such devices exhibit stable performance and long lifetimes. However, these integrated devices generally employ bulk materials and the sizes of such devices are thus huge. Inevitable electronic losses, more precisely lower conversion rates are often noticed during the transmission processes through the external circuit connection. As for the concept of a photo-assisted or photo-driven energy storage device, it does not really fit because it simply connects two devices together.

Type II: Three-electrode devices with the introduction of photoelectrodes

This type is the fusion of two devices. It is only the one that simultaneously completes the photoelectric conversion and energy storage. This device is usually composed of a positive electrode, a negative electrode, and a photo electrode **(Figure 3g)**. Since the photo electrode is usually from semiconductors or photosensitive materials, these devices realize the direct conversion of the photoelectric energy on the photo electrode and subsequent electron transfer

to complete the energy storage. The sizes of such devices are relatively small. Energy conversion is done directly inside the batteries that further improve the energy conversion rate and reduce the energy loss of these devices as well reduce their integration costs.

Type III: Two-electrode devices based on dual-functional materials

This type is a two-electrode device, where the photoelectrode features the functions of both photo-electric conversion and energy storage. The photoelectrode plays a key role and is the core part of the whole device. Another electrode is an ordinary battery cathode/anode, ensuring the balance of electron transfer throughout the device **(Figure 3h)**. Compared with other devices, these devices are more efficient in energy transfer, simpler in device construction, and lower in overall cost. However, the design of the photoelectrodes for these devices is more challenging. Up to the properties of the employed photoelectrodes or different photo-active materials, these devices own different conversion mechanisms and working mechanisms.

3. Performance of photo-assisted energy storage devices

3.1 Photo-assisted SCs

The SCs are very suitable for large-area energy storage, owing to ultrahigh power densities, quick response to potential changes, long cycle life, and high safety of these outstanding electrochemical energy storage devices.[53–55] The solar charged SCs systems have thus gained popularity over the past years, especially with the development of photoelectrode materials that can simultaneously store electrochemical energy and harvest light. In 2004 the design of the first light-assisted SCs was reported and so-named a photo capacitor.[15] Compared with a traditional SC, this device had one more photoelectrode. This photoelectrode was composed of dye-sensitized semiconductor nanoparticles, a hole-trapping layer, and activated carbon particles that were in contact with an organic electrolyte solution. Charges that were generated through light harvesting were directly stored in an SC. Such a photoelectrode efficiently improved the specific capacitance of the SC (with a factor of 50%) and had good cycle

performance. Since then, various light-assisted energy storage devices have been proposed and fabricated. For example, novel materials were employed and combined[56] to construct integrated perovskite solar capacitors. They were formed by stacking a solid-state photo capacitor (~1 μm), $CH_3NH_3PbI_3$ photoactive and multi-junction perovskite solar cell in the form of layer by layer (**Figure 4a**). This device exhibited an excellent areal capacitance of 2.35 mF cm^{-2} and a photo-chemical-electricity energy conversion efficiency as high as 25%. For the first time, the layer of perovskite bulk and interfacial defects were taken into account during mathematic simulations of the performance of this device. In more detail, the simulation took into account each individual layer of the bandgap energy of the photo-assisted SC, valance and conduction bands, carrier mobility, and carrier density. It revealed a 14-order increase in its recombination rate over perfect perovskite structure. The performance of this perovskite SC is moderately vulnerable to both internal and external triggers, according to the results of its areal capacitance (**Figure 4b**), output voltage (**Figure 4c**), and photo charging efficiency under different lighting conditions, and frequencies. This ultra-thin and robust architecture was believed to have the potential the usage in wearable and portable flexible electronics.

Metal oxides and hydroxides (e.g., RuO_2, Fe_2O_3, NiO, MnO_2) have been widely explored to construct different SCs. The driving force is that their specific capacitances are relatively high and even approachable to their theoretical values very recently. Meanwhile, their cycle life is long.[57–60] It is known that energy storage of these metal oxides mainly relies on the diffusion of electrons between oxide layers as well as the binding of ions between intercalation sites. Namely, metal oxides react with ions to form intermediate compounds. Subsequently, their crystal structures are changed and accordingly, the metal valence states are altered. Importantly, some metal oxides (e.g., TiO_2, ZnO, Cu_2O)[61–63] contribute to both the capacity of an SC and the PV properties of the device at a specific light wavelength. In this way, a photoelectrochemical battery-type SC was designed and reported.[64] The electrode was prepared by use of a Fe_2O_3@$Ni(OH)_2$ core-shell nanorod array **(Figure 4d)**. Under light illumination, Fe_2O_3 absorbs solar energy and creates electron-hole pairs. Meanwhile, $Ni(OH)_2$ is oxidized to NiOOH by the photo-generated holes **(Figure 4e)**. A Fe_2O_3 array photoelectrode

was further coated with a 6-nm thick $Ni(OH)_2$ shell layer in order to totally block the side-reaction of water oxidation. Consequently, this Fe_2O_3@$Ni(OH)_2$ photo-assisted SC showed a specific capacitance of 20.6 mF cm^{-2} at a current density of 0.1 mA cm^{-2}. The specific capacitance retained about 66% after 1000 charging/discharging cycles at a scan rate of 50 mV s^{-1} **(Figure 4f)**. A photo-electrode was also developed using the unique properties of metal oxides.[63] The photoelectrode was fabricated using a light-sensitive material with a hierarchical nanostructure **(Figure 4g)**, namely the copper foam-supported copper oxide/nickel copper oxide nanosheet arrays (CF@CuOx@NiCuOx NAs, **Figure 4h**). During the light irradiation with a light output of 1.76 W, the as-fabricated NAs showed a high areal specific capacity of 2.64 F cm^{-2} at a current density of 5 mA cm^{-2}, which was 44.8% greater than the capacity attained without light illumination **(Figure 4i)**. The combination of photosensitive Cu_2O and pseudoactive NiO components was suggested to be responsible for such photo-enhanced charge storage performance and achieved an improved capacity of energy storage devices. However, the increased capacity still leaves a lot of room for improvement, as it possesses unstable rate performance during high current charging and discharging processes, due to the involvement of metal oxides. Especially, it is instable during sun charging processes.

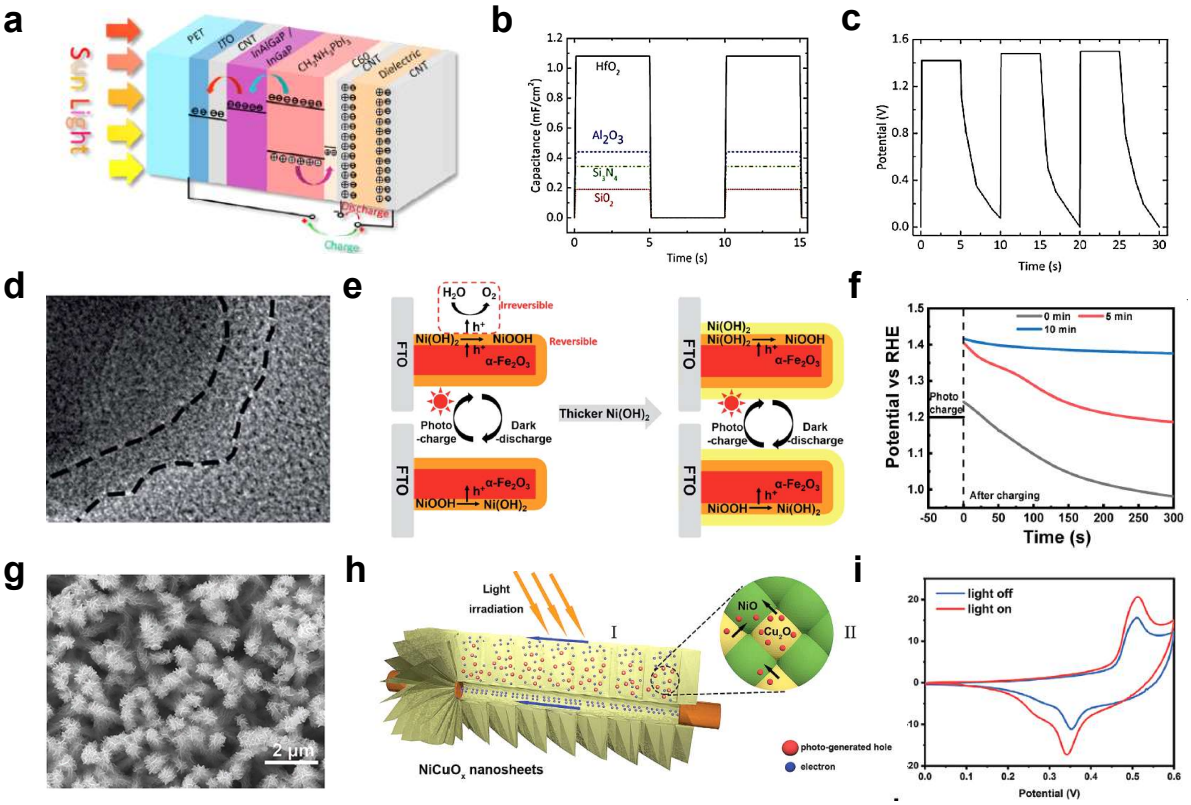

Figure 4. Examples of photo-assisted SCs. (a) Schematic of the designed Perovskite Photo-capacitor (PPC). (b) the GCD curves of this PPC under the different active illumination areas. (c) The GCD curves of this PPC based on the active illumination area of 9.06×10^{-9} cm^2. Reproduced with permission.[56] Copyright 2019, Elsevier. (d) The high resolution transmission electron microscopy (HR-TEM) images of Fe_2O_3@$Ni(OH)_2$ where the deposition time of $Ni(OH)_2$ was 10 min. (e) Schematic of photo-charging and dark discharging processes on Fe_2O_3@$Ni(OH)_2$ with different thicknesses of $Ni(OH)_2$. (f) Open circuit potentials of the device with different times for the deposition of $Ni(OH)_2$. Reproduced with permission.[64] Copyright 2018, Royal Society of Chemistry. (g) The scanning electron microscopy (SEM) image of the CF@CuOx@NiCuOx NAs. (h) The schematic illustration of thus photoelectrochemical material. (i) The CVs of the CF@CuOx@NiCuOx NAs at a scan rate of 2 mV s^{-1}. Reproduced with permission.[63] Copyright 2021, Wiley-VCH.

In addition to individual SCs and batteries, hybrid SCs have appeared as a new type of energy storage device. They are a simple combination of a battery-type electrode and a capacitor-type electrode and are expected to fully integrate the advantages of both batteries (more exactly high energy densities and long discharge times) and SCs (more exactly high power densities and short charge times). Therefore, hybrid SCs bridge the gap between batteries and SCs for energy storage.[65,66] Among various hybrid SCs, metal ion hybrid SCs have been extensively studied. For example, zinc ions have been utilized to assemble efficient and safe aqueous zinc ion hybrid SCs, thanks to their low costs, high reduction potential (−0.76 V, relative to a standard hydrogen electrode), and environmentally friendly properties.[67,68] The photo-assisted zinc-ion SC is even more promising in that it offers a high energy density, a high power density, and long cycle life. In this regard, it is expected that it can be used in a wide range of applications, from portable electronics, and electric vehicles, to grid-scale energy storage. In the first-time reported photo-assisted zinc-ion capacitor (ZIC),[20] 2D graphitic carbon nitride (g-C_3N_4) was used as both a capacitor electrode and a light-collecting material to simultaneously store charges and harvest solar energy **(Figure 5a)**, respectively. The continuous operation under a photo-powered mode

showed a photo charge specific capacitance of up to 11377 mF g^{-1}, a photo charge voltage response of ~850 mV that maintained about 90% capacity even over 1000 charging/discharging cycles at a current density of 15 mA g^{-1}. Since this device owned a simple architecture compared to alternative solutions using the combination of the PV and energy storage systems, it was expected to be used to power ultra-low power compact off-grid devices, for example in internet of things (IoT) applications. Later, an improved photo-ZIC system[69] was reported using the photoanode from vanadium oxide (V_2O_5) nanofibers and silver nanowires as well as a cathode from activated carbon **(Figure 5b)**. Compared with the previous photo-ZIC devices,[20] the photo charge energy density of this device was increased by 7 times (from ~ 0.7 to ~ 4.8 Wh kg^{-1}). Its capacity was improved 12 folds (from ~ 11.4 to ~ 138 F g^{-1}). The device maintained its capacity of 99% after 4000 charging/discharging cycles in both dark and illumination conditions. In this study, silver nanowires outperformed carbon-based conductive additions, because they facilitated the transport of photo-excited holes and offered light scattering centers that improved the absorption efficiency of visible light. There exist many challenges for light-assisted SCs. For example, they exhibit rapid charging rates. However, in many instances, the utilization of aqueous electrolytes leads to narrow potential windows and consequently lower energy densities of as-contracted devices. Furthermore, the practical applications of aqueous electrolytes are limited to narrower temperature ranges. It tends to evaporate more quickly under light, potentially leading to a shortened lifespan.

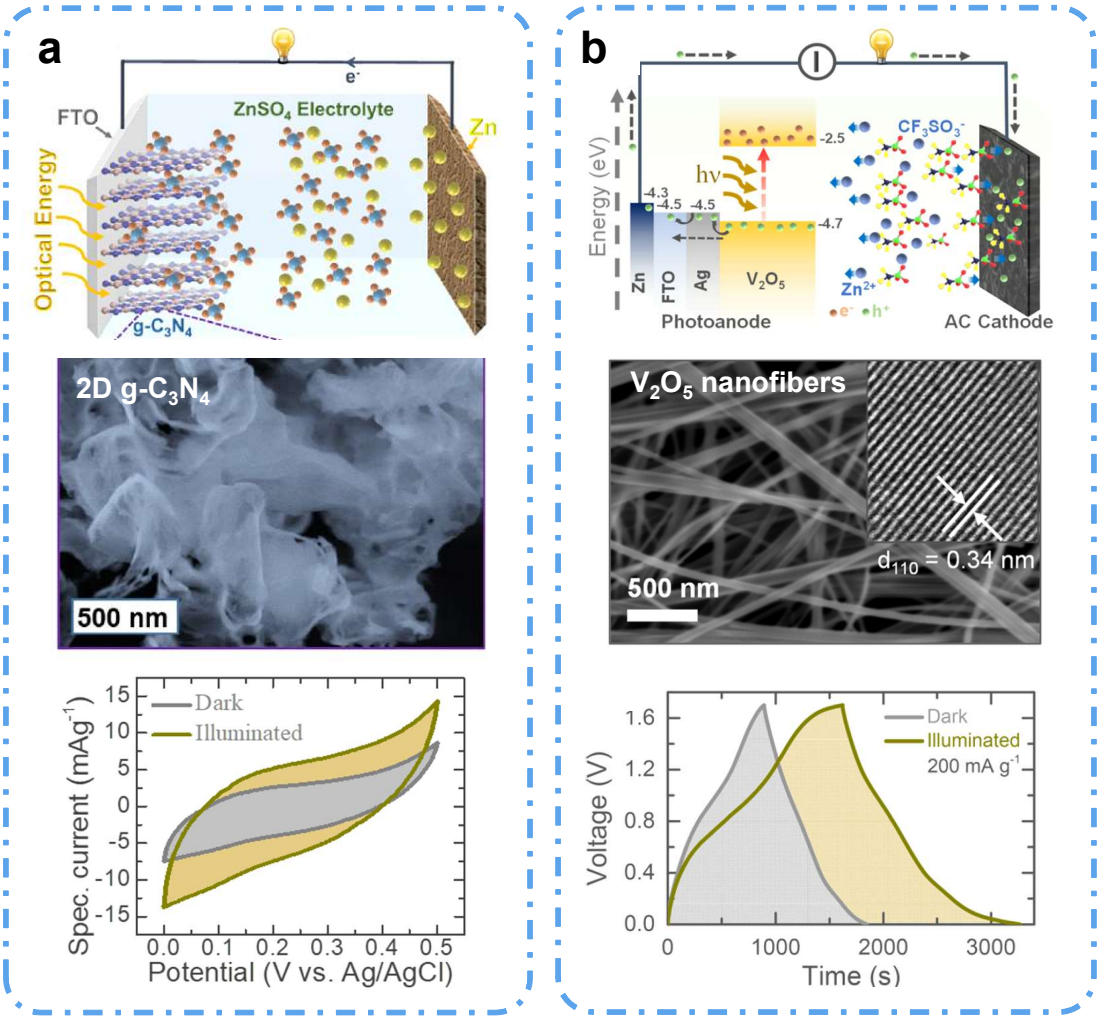

Figure 5. Examples of photo-assisted hybrid SCs: Schematic illustration, images of photoelectrochemical materials and their electrochemical performances of a photo ZIC (a) using a 2D g-C_3N_4 cathode and a Zn anode[20] and (b) using an Ag@V_2O_5 photoanode and a cathode of active carbon.[64] Reproduced with permission.[20] Copyright 2020, American Chemical Society. Reproduced with permission.[69] Copyright 2020, American Chemical Society.

3.2 Photo-assisted lithium-metal batteries

Lithium-ion batteries (LIBs) have been proved to own superior performance, such as long cycle life, high energy densities, and no memory effects. They actually stand out from the crowd of various energy storage devices and have successfully become the first commercialized secondary battery system.[70,71] Different from these traditional LIBs, there are new research

interests in LIBs have been triggered, namely to utilize the LIBs to store electrical energy that is directly converted from solar energy. Under such a concept, energy conversion can be accomplished more efficiently and meanwhile energy consumption can be reduced during the process.[72] Light-assisted lithium-ion batteries incorporate light-absorbing materials into an electrode structure to form a photoelectrode, typically the cathode.[73,74] The light-absorbing material receives the photons to produce electron-hole pairs, the electrons are excited to a higher energy state and then the electrons are transferred through the electrode material to flow in an external circuit to the anode. The transferred electrons from the light-absorbing material combine with lithium ions from the electrolyte, resulting in the deposition of lithium metal or lithium compounds. During discharging, the lithium ions are released from the anode and move back to the cathode, generating electrical energy that can be used to power devices. The light-absorbing materials do not directly participate in the discharging process and act as catalysts for the charging process. For such light-assisted energy storage devices, light-active photoelectrode materials, redox mediators, or dyes have been incorporated into different batteries. Among various light-active photoelectrode materials, Nano-Cu_2S is an important example. This semiconductor owns a wide energy band gap and is thus widely used in solar cells (e.g., dye-sensitized solar cells and quantum dot-sensitized solar cells).[75,76] Meanwhile, Cu_xS (e.g., CuS, Cu_2S) is one of the potential anode materials for the construction of the LIBs, due to its high specific capacity, low price, and environmental friendliness.[77] For example, bi-functional Cu_2S was chosen as the shared electrode to construct a two-electrode light-assisted rechargeable battery,[78] where the tedious energy conversion process was avoided**.** In more detail, the electrode was made by direct deposition of a Cu_2S counter electrode onto an N719 light-sensitive TiO_2 photoanode (TiO_2/dye/Cu_2S). This electrode enabled lithium ions to lithiation and delithiation. Meanwhile, it harvested the light to produce dye^+ molecules and electrons, and further integrated photoelectric conversion and energy storage into a single electrode. In this integrated system, Cu_2S performed superbly as a shared electrode in terms of capacity, stability, and compatibility. The charging potential of this two-electrode light-assisted rechargeable cell was reduced to 0.2 V, while it was chargeable under the light illumination.

More importantly, solar illumination boosted the charging capacity by a factor of almost two. The discharging capacity was significantly and consistently increased when the gadget was lit during the discharging process. The electron generation, transfer, and storage mechanism were expected to hold great promise for potential applications (e.g., practical photo-chargeable batteries). Another frequently used semiconductor material is V_2O_5, which has been integrated into LIBs and zinc-ion batteries (ZIBs).[79] The capacities of these integrated devices were greatly improved under the light irradiation. The photocathodes in light-assisted ILBs were made of vanadium pentoxide nanofibers that were blended with poly(3-hexylthiophene-2,5-diyl) (P_3HT) and reduced graphene oxide (rGO) additives **(Figure 6a)**. The photo charge separation and transmission mechanism required for the recharging were supported by these photocathodes. This photo LIB exhibited the capacity improvement of over 57% when illuminated **(Figure 6b)**. They were possible to be charged to a voltage of 2.82 V with the aid of light, achieving conversion efficiencies of 2.6% and 0.22% under the illumination of a 455-nm light and sun light, respectively. Due to the better synergistic effects of these materials, the device has a higher capacity and conversion efficiency, but the cycling performance can be less than the optimal one. This is because the mechanical mixing of the materials results in poor contact. A better integration of the photosensitive and electroactive materials is thus a challenge to overcome.

As alternative active materials to semiconductors, redox-active organic compounds have been integrated into rechargeable batteries. This is because some organic compounds fall within the category of semiconductors and thus absorb visible light. Moreover, they have the capacity to store charges. All these characteristics result in the applications of organic compounds as potential photo-charging active substances. Additionally, they feature various benefits over typical inorganic metal oxide-based materials, including safety, potential costs, and renewability. It must highlight here that the twin properties of organic molecules - charge storage and light harvester - have been seldom considered in previous studies. In one study, organic small molecules (e.g., lithiated tetrakislawsone) were mixed with other materials to fabricate lithium-ion electrode materials.[80] In this case, organic small molecules were used as

active materials to store lithium ions as well as photoactive materials to harvest light **(Figure 6c,e)**. These molecules absorbed sunlight to generate electron-hole pairs, leading to reductive deposition of lithium ions and the occurrence of oxidation reactions. This device exhibited significantly increased performance with respect to its specific capacity and coulombic efficiency under the light illumination **(Figure 6d)**. Further tuning of the band gaps of the molecules varied the absorption of the light at specific frequencies, which was stated to be a new strategy to design light-assisted batteries. Designing and optimizing effective organic cathodes for systematic compatibility and simple assembly remains challenging. With this challenge, a C60 inside porous organic cage (C60@POC) was designed to constructed a photo-assisted Li-organic battery.[81] It demonstrated improved photovoltaic conversion and storage efficiency, which was largely attributed to the rapid charge separation and accelerated reaction kinetic of C60@POC **(Figure 6f)**. Under illumination, the device exhibited increased solar to electrochemical energy conversion (~1%) and round-trip efficiency (24.2%). In addition, the discharge/charge voltage and output/input power were raised/lowered by 470/410 mV and 81.4%/13.2% respectively **(Figure 6g)**. In addition, there have been some efforts on photo-assisted lithium batteries in recent years,[82–84] such as the use of photo-assisted lithium deposition/stripping process to achieve uniform Li deposition, to reduce the formation of lithium dendrites and entually to obtain a more stable lithium-ion battery[82], and to apply a self-powered lithium-ion battery based on LiV_2O_5 as the photocathode without the addition of photosensitive materials.[83] Although the photo-assisted Li-ion batteries have performed the desired photo-electronic conversion and storage capability, their low conversion and efficiencies still severely limit their practical applications.

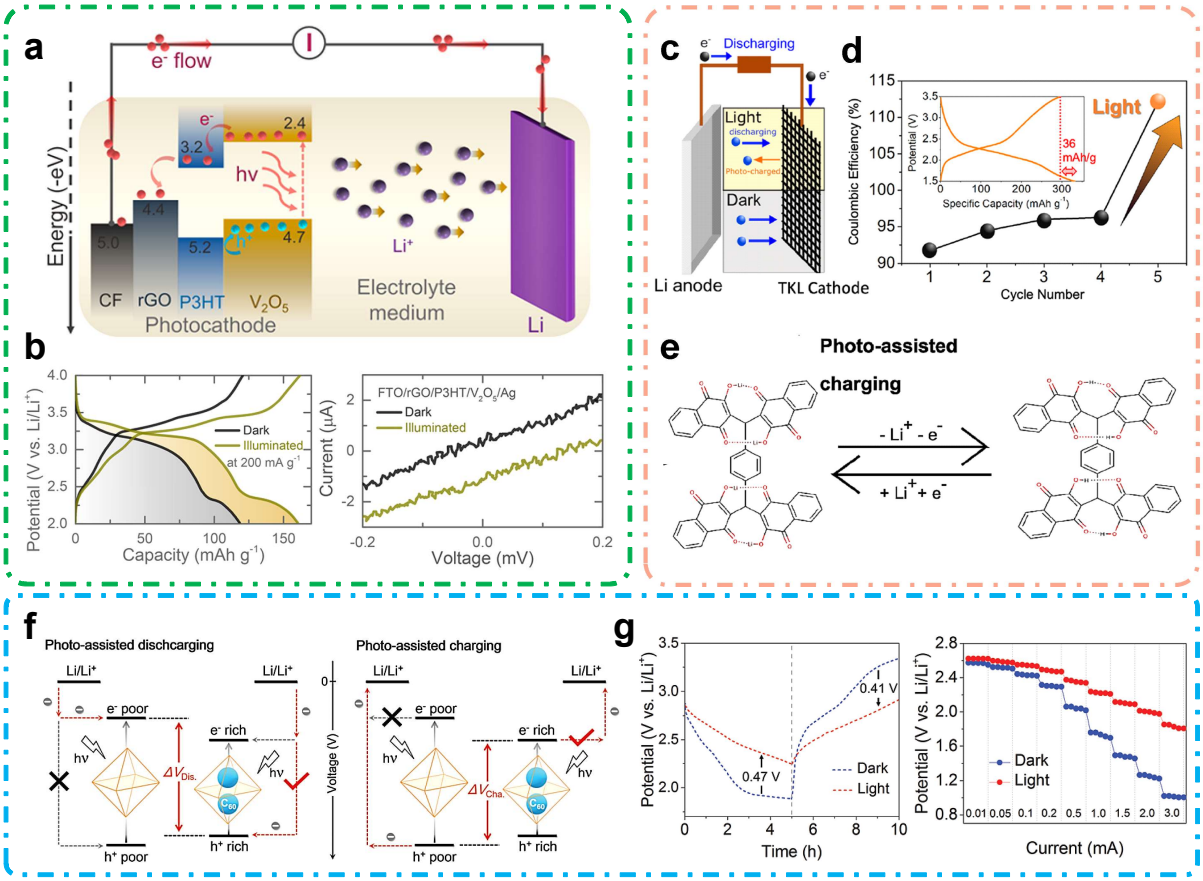

Figure 6. Examples of photo-assisted LIBs. (a) Energy band diagram, (b) the GCD curves at a current density of 200 mA g^{-1} and I-V curves under illumination in dark of an FTO/rGO/P_3HT/V_2O_5/Ag photodetector. Reproduced with permission.[79] Copyright 2021, American Chemical Society. Schematic representation of photo discharging (c) and charging (d) as well as coulombic efficiency in dark and light conditions (e) of a photocharging battery using tetrakislawsone as a cathode. Reproduced with permission[80]. Copyright 2021, American Chemical Society. (f) Schematic diagram and (g) photoelectrochemical energy storage performance of the photo-assisted Li-organic battery with POC and C60@POC cathodes. Reproduced with permission.[81] Copyright 2022, Royal Society of Chemistry.

In addition to these different PV cells, many different battery concepts have been developed on the battery side. For example, lithium-O_2 (Li-O_2) batteries have attracted especial attention. Due to their ultra-high theoretical energy densities (about 3500 Wh Kg^{-1}), they have been considered as the most promising next-generation high-specific energy storage systems.[86,87] To eventually

produce Li-O_2 batteries with high specific capacity, high power, and long-term stability (or cycling Li-O_x batteries), the biggest challenge that has to be overcome is to avoid the side reactions since they enhance the overcharge potential and impair the cycling performance of Li-O_2 batteries. Interestingly, light-assisted charging effectively reduced the overpotential of the Li-O_2 cells. In a bi-functional photo-assisted Li-O_2 system that was constructed using a hierarchical TiO_2-Fe_2O_3 heterojunction,[88] the photogenerated electrons and holes were found to play crucial roles in lowering the overpotentials in the discharging and charging processes, respectively **(Figure 7a)**. The dense surface electrons of the cathode under illumination changed the shape of the discharge product (Li_2O_2), resulting in accelerated breakdown kinetics of Li_2O_2 during the charging process. Consequently, the input and output energies of such a battery were adjustable under light illumination. A very low overpotential between the charging and discharging plateaus of 0.19 V was achieved together with a retaining efficiency of 86% after 100 discharging/charging cycles at a current density of 0.01 mA cm^{-2}.

It has been recently demonstrated that light-assisted charging effectively improves the performance (e.g., cycle stability) of Li-CO_2 batteries. The Li-CO_2 batteries have attracted lots of attention in that they use CO_2 as the energy carrier, of which energy density is as high as 1876 Wh kg^{-1}. Namely, the Li-CO_2 batteries have the characteristics of both CO_2 conversion and energy storage. Their main obstacle is slow CO_2 reduction/release kinetics at the anode, seriously hindering the practical applications of the Li-CO_2 batteries. To overcome the polarization problem of traditional Li-CO_2 cells, the SiC/rGO hybrid was employed as the cathode of a light-assisted Li-CO_2 battery **(Figure 7b)**.[89] In this case study, SiC absorbed photons and then produced high-energy electrons that were transferred by rGO. The recombination of photogenerated electrons was thus efficiently prevented. These photogenerated electrons accelerated the kinetics of CO_2 reduction reactions during the discharging process. The discharge voltage of this battery was raised up to 2.77 V, extremely close to the theoretical potential (2.80 V) of the reaction of $4Li + 3CO_2 \rightarrow 2Li_2CO_3 + C$. Meanwhile, the holes made on the photoelectrode during the charging process encouraged the breakdown of Li_2CO_3, leading to reduced overpotential of the Li-CO_2 battery. The energy

efficiency of this battery was as high as 84.4%. In another report, a carbon nanotube coated carbon nitride layer with nitrogen defects (CNT@C_3N_4) heterostructure photocathode was designed **(Figure 7c)**.[90] Such a cathode integrated both photoelectric effect and unique defective structure of C_3N_4, where the kinetics of CO_2 reduction/release reactions was much accelerated. The incident light excited high-energy photoelectrons/hole pairs in C_3N_4 and the reaction potential barrier were then overcome. An enhanced electric field was induced around C_3N_4 for the efficient separation/transfer of photogenerated carriers and thermodynamically favorable reaction pathways. The obtained Li-CO_2 cell exhibited a round-trip efficiency 98.8 % and superior cycling stability of 86.1% after 100 charging/discharging cycles at a current density of 0.02 mA cm^{-2}. Its multiplicative performance was stable, even at a current density of 2.0 mA cm^{-2}.

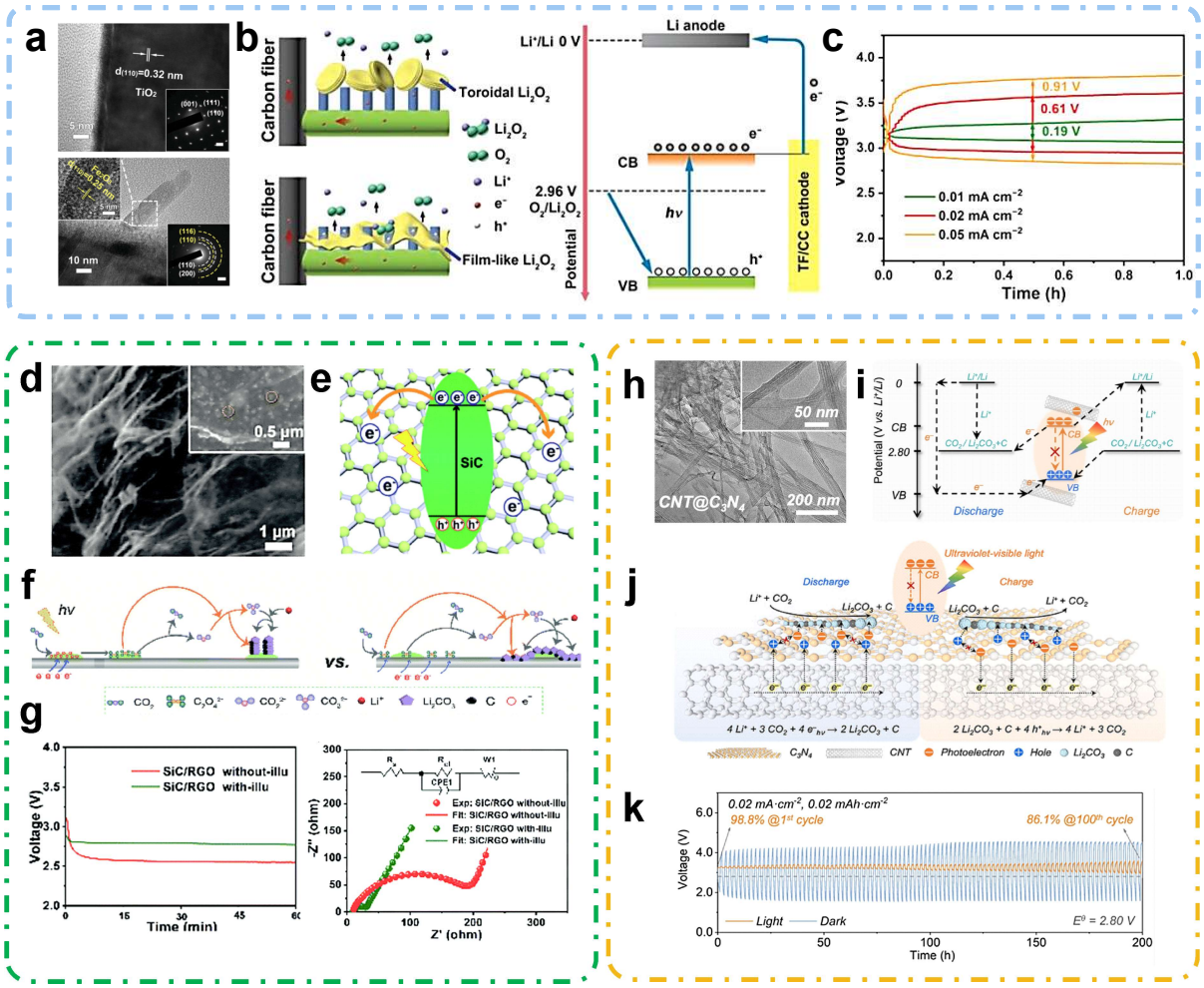

Figure 7. Examples of Li-O_2 and Li-CO_2 batteries: (a) TEM image of a TiO_2/CC cathode, (b)

Schematic illustration the charging process with and without illumination and (c) GCD curves of at different current densities of the Li–O_2 battery. Reproduced with permission[88]. Copyright 2020, Wiley-VCH. (d) SEM images, (e,f) Diagrammatic representation of the combinatorial impact of the SiC/rGO nanocomposite and (g) electrochemical performance of a Li-CO_2 battery using a SiC/rGO cathode. Reproduced with permission.[89] Copyright 2020, Royal Society of Chemistry. (h) TEM images of a CNT@C_3N_4 heterostructure, (i,j) Schematic illustration the charging/discharging process and (k) subsequent cycling profiles in the light and dark of a Li-CO_2 battery using a CNT@C_3N_4 photocathode. Reproduced with permission.[90] Copyright 2022, Wiley-VCH.

In addition to Li-O_2 and Li-CO_2 batteries, rechargeable lithium-iodine (Li-I_2) batteries have been proposed as promising candidates for energy storage modules in integrated photo-rechargeable batteries. The advantages of the Li-I_2 batteries include their low costs and high abundance of elemental iodine (eg., 50 – 60 mg L^{-1} in oceans).[91,92] Moreover, the energy level of I_2 well matches with most of light-absorbing materials in the integrated system.[93] For example, a hybrid I_2/N719-dye/TiO_2 composite has been used as a dual-functional photoelectrode in an integrated, photo-assisted, and rechargeable Li-I_2 battery system **(Figure 8a)**.[94] The photovoltage of this hybrid photoelectrode balanced the charging voltage of the cell. It reduced the charging potential about 100 mV during a chronoamperometric test. More specifically, under light illumination of this solar-integrated Li-I_2 battery, its charging/discharging capacity was increased from 171/166 mAh g^{-1} to 204/193 mAh g^{-1}. Its energy efficiency (namely the ratio of the output electric energy to the input electric energy) was 93%, higher than that of an individual Li-I_2 battery. The density functional theory (DFT) calculations proved that the superior performance of this solar-integrated Li-I_2 battery stems from increased redox kinetics of lithium polyiodide conversion reactions.

Lithium-sulfur (Li-S) battery is another extremely promising energy storage device, thanks to its ultra-high theoretical energy density as well as wide and cheap source of raw sulfur materials.[95,96] Unfortunately, the severe shuttle of polysulfides and the lagging reaction

kinetics hinder the industrial applications of Li-S batteries. As shown in the previous session, the introduction of light into Li-O_2 and Li-CO_2 cells reduces the charge voltages and achieves ultra-high discharge voltages. In other words, the addition of light speeds up the electrochemical kinetics in a secondary battery. In this regard, the sulfur redox reactions are predicted to be accelerated and the charging/discharging energy barriers of a Li-S battery that is expected to be reduced once the photocatalysis is integrated. For such integrated Li-S batteries, the shuttle effect is promising to be suppressed and the kinetics of the overall electrochemical processes are possible to be efficiently improved.[97] The photo-generated carriers might boost the carrier density of the overall battery system, resulting in faster and more thorough charging/discharging reactions. Based on these assumptions, a CdS-TiO_2/carbon cloth was employed as a multifunctional cathode to construct a photo-assisted Li-S battery **(Figure 8b)**[98]. Under light illumination, this PV electrode produced a catalytic effect together with a photoconductive effect. The former reduced the reaction energy barrier for the conversion of polysulfide to lithium sulfide, while the latter produced a large number of carriers and increased the charge concentration inside the device. This light-assisted cell exhibited excellent electrochemical performance (e.g., the capacity up to 1225 mAh g^{-1}, 10% higher than that without light assistance) since the deposition of lithium sulfide (Li_2S) was decreased from 2.15 to 2.08 V. The cycling performance of such a cell was stable. This research was believed to offer a fully sustainable strategy to effectively enhance the chemical capability of Li-S batteries. Recently, dye-sensitized solar cells were integrated with the Li-S batteries to construct high-performance photo-assisted rechargeable Li-S batteries **(Figure 8c)**.[99] A bridge to achieve the dual functions of photoelectric conversion and storage was provided by a compatible C/S electrode. A new electrolyte – lithium bis((trifluoromethyl)sulfonyl)azanide (LiTFSI) was further designed and synthesized. In contrast to the dual electrolytes that were previously applied in the photo-assisted rechargeable batteries, this electrolyte facilitated charge separation and improved the capacity and stability of this integrated photo-assisted rechargeable battery. Under light illumination, the adjustment of the photogenerated carrier led to a 0.12 V-drop of the charge voltage of this photo-assisted Li-S battery as well as the rise of discharge capacity up to 885

mAh g^{-1}. Compared to other lithium metal batteries, the sulphur cathode material in Li-S batteries has a higher absorption of light, which can improve the performance and response of the battery. Meanwhile, the introduction of light can cause the interference with the photoelectrochemical reactions in the device, resulting in the loss of electrons and ions or the formation of by-products of the reaction. It is important to note that the exact impact of the introduction of light into a Li-S battery depends on the cell design, material selection and lighting conditions. Therefore, in practical applications, the effect of light on the performance of the Li-S battery must be carefully considered and appropriate measures must be taken to achieve optimum cell performance.

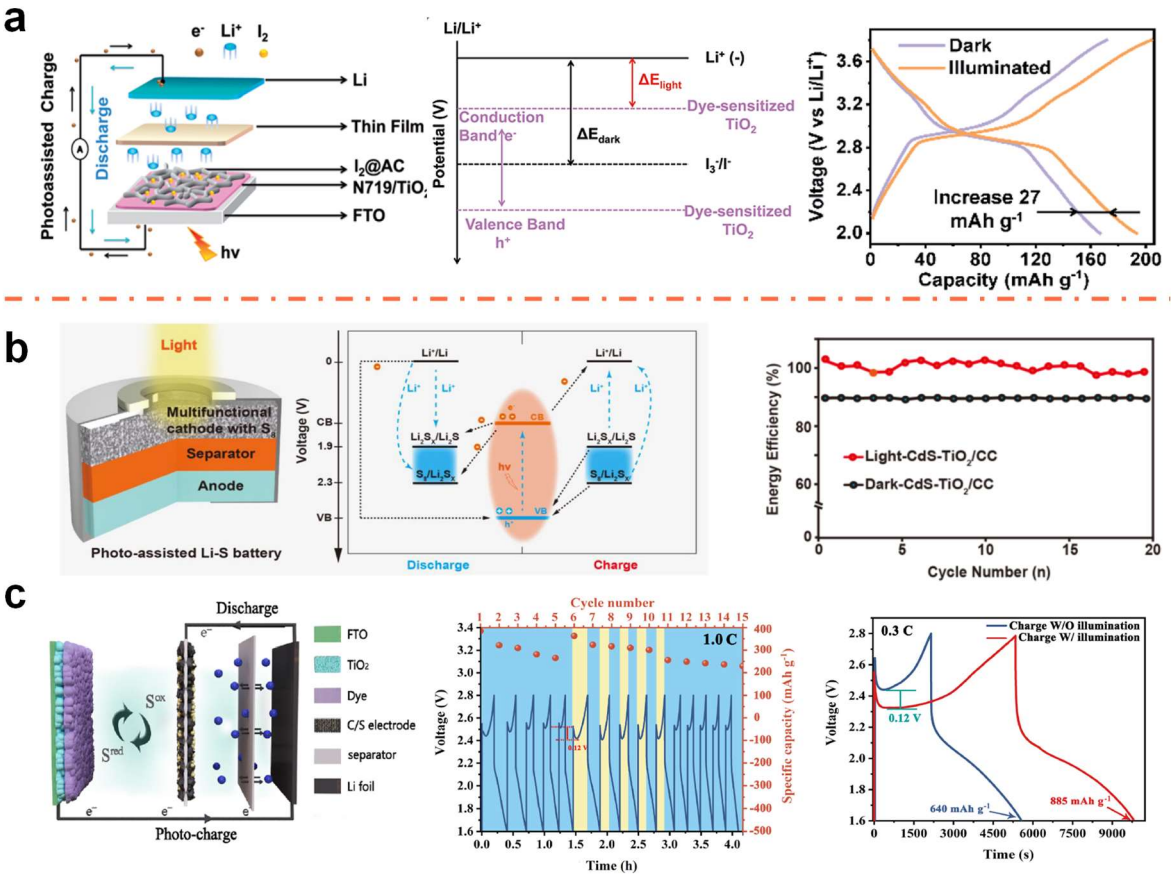

Figure 8. Examples of Li-I_2 and Li-S batteries: (a) Schematic configuration, (b) energy band diagram and (c) the GCD curves of a photo-assisted rechargeable Li-I_2 battery at a current density of 100 mA g^{-1} in dark and under illumination. Reproduced with permission.[94] Copyright 2022, Royal Society of Chemistry. (d) Working mechanism and (e) energy

efficiencies of a photo-assisted Li-S battery using a CdS-TiO_2/CC electrode. Reproduced with permission.[98] Copyright 2022, Elsevier. (f) Device diagram, (g) the cycling performance with alternating light-assisted and dark charging, and (h) the GCD curves of a photo-assisted rechargeable Li-S battery at a current density of 500 mA g^{-1} with and without light illumination. Reproduced with permission. [99] Copyright 2023, Elsevier.

3.3 Photo-assisted zinc-metal batteries

In the post-lithium era, zinc (Zn) metal has been proposed as a promising metal anode, stemming from its high specific capacity (= 820 mAh g^{-1}), low redox potential (= −0.76 V *vs*. standard hydrogen electrode, SHE), abundant reserves, and low cost.[100] Above the standard design and development of zinc ion batteries (ZIBs), recently more focus has been laid on the assembling of light-assisted ZIBs. In 2020 the first photo-rechargeable ZIB (photo-ZIB) was reported, where sunlight was directly collected for the charging of a ZIB.[21] The photosensitive cathode consisted of a mixture of V_2O_5 nanofibers, P_3HT, and rGO. With aid of a photodetector, transient absorption spectroscopy, and electrochemical analysis, the performance of this device was compared in dark and under light illumination **(Figure 9a)**. The capacity of the V_2O_5 cathode was about 190 and 370 mAh g^{-1} in dark and under light illumination, respectively. Its photoconversion efficiency was about 1.2%. Later, several photoelectrodes were fabricated by physical combination of electrode materials with conductive additives, charge transfer materials, and binders. Then they were simply cast on a current collector. Note that these processes are easy to scale up. However, randomly mixing photocathode materials with a charge transfer material and non-conducting binder might lead to poor separation and transport of photo charges. Therefore, energy conversion efficiencies of these photoelectrodes were relatively low in most cases. Differently, a carbon fiber current collector was coated with zinc oxide (ZnO) as a hole-blocking and electron transport layer, followed by the direct growth of vanadium dioxide (VO_2) material **(Figure 9b)**[101]. In comparison to an earlier work using a mixed VO_2 photocathode, the interface and charge separation of this carbon fiber based photoelectrode was improved, enabling an increase in the photo-conversion efficiency (namely from 0.18% to

0.51%). After 500 charging/discharging cycles at a current density of 1000 mA g^{-1}, the capacity retention of 73% was obtained. Different from previously reported photo-charged ZIBs, where either V_2O_5 or VO_2 was mainly applied as the photoactive cathode, a simple mixture of VO_2 and rGO was employed as a photo cathode.[102] Under light illumination, the created internal electric field between VO_2 and rGO was sufficient to transport electrons from VO_2 to rGO as well as to separate photogenerated electrons and holes. According to its energy band diagram **(Figure 9c)**, the creation, separation, and transportation of electron/hole pairs were clearly demonstrated: electrons transfer from VO_2 to rGO and then to FTO, while holes from VO_2 to the Ag electrode. Such a photo-ZIB utilized the light to charge this device and further increase its capacity. For example, at a current density of 200 mA g^{-1}, its capacity was 282 and 315 mAh g^{-1} in the dark and under light illumination, respectively. This photo-ZIB also showed high-rate performance under light illumination. Instead of such drop-coating/mixing methods, the photo-ZIBs have been developed by starting with carbon felt collectors. For example, the ZnO films were synthesized on the top of carbon felt collectors. These films were then directly used as electron transport and hole-blocking layers.[103] Subsequently, the MoS_2 layers were deposited, which took care of both generating photogenerated electron/hole pairs and storing Zn ions. Since the band gap of MoS_2 (~1.9 eV) is smaller than that of V_2O_5 (~2.2 eV) and VO_2 (~2.3 eV), MoS_2 matches better the solar spectrum **(Figure 9d)**. In this way, the overall solar conversion efficiency of the device was improved. In addition, previous reports on photo-charged cells usually adopted toxic materials (e.g., Pb, V_xO_y), whereas MoS_2 is a harmless material. Some aqueous ZIBs were recently combined with perovskite solar cells.[104] The anode of such a zinc battery was zinc metal and its cathode was a hetero-structural Co_2P-CoP-$NiCoO_2$ nanoarray (**Figure 9e**). The electrode material was *in situ* grown on one hydrophilic side, which has better compatibility and infiltration for aqueous electrolytes (**Figure 9f**). Another hydrophilic side served as the counter electrode of the perovskite solar cell to obtain better interfacial contact. The cathode electrode material and the perovskite light absorber material in the solar cell formed a sandwich structure, leading to improved electron transmission (**Figure 9g**). Such an assembled device exhibited intentional electrochemical performance **(Figure 9h)**.

After 25000 charging/discharging cycles at a current density of 32 A g^{-1}, the capacity of this cell was still maintained at about 78% of its initial value. It showed a high-power density of 54 kW kg^{-1} at a current density of 32 A g^{-1} and a high energy density of 366 Wh kg^{-1} at a current density of 2 A g^{-1}. The voltage range was limited within 1.40 – 1.90 V, exhibiting an efficiency of about 6%. The device has shown great potential for practical applications as it can cope with irregular changes in current due to the fluctuations in current caused by the intensity of light when absorbing sunlight. It has demonstrated excellent rate and cycling performance. The Zn metal batteries are also less expensive and safer than Li-ion batteries. Furthermore, the aqueous electrolyte avoids the biggest safety issue - thermal runaway.

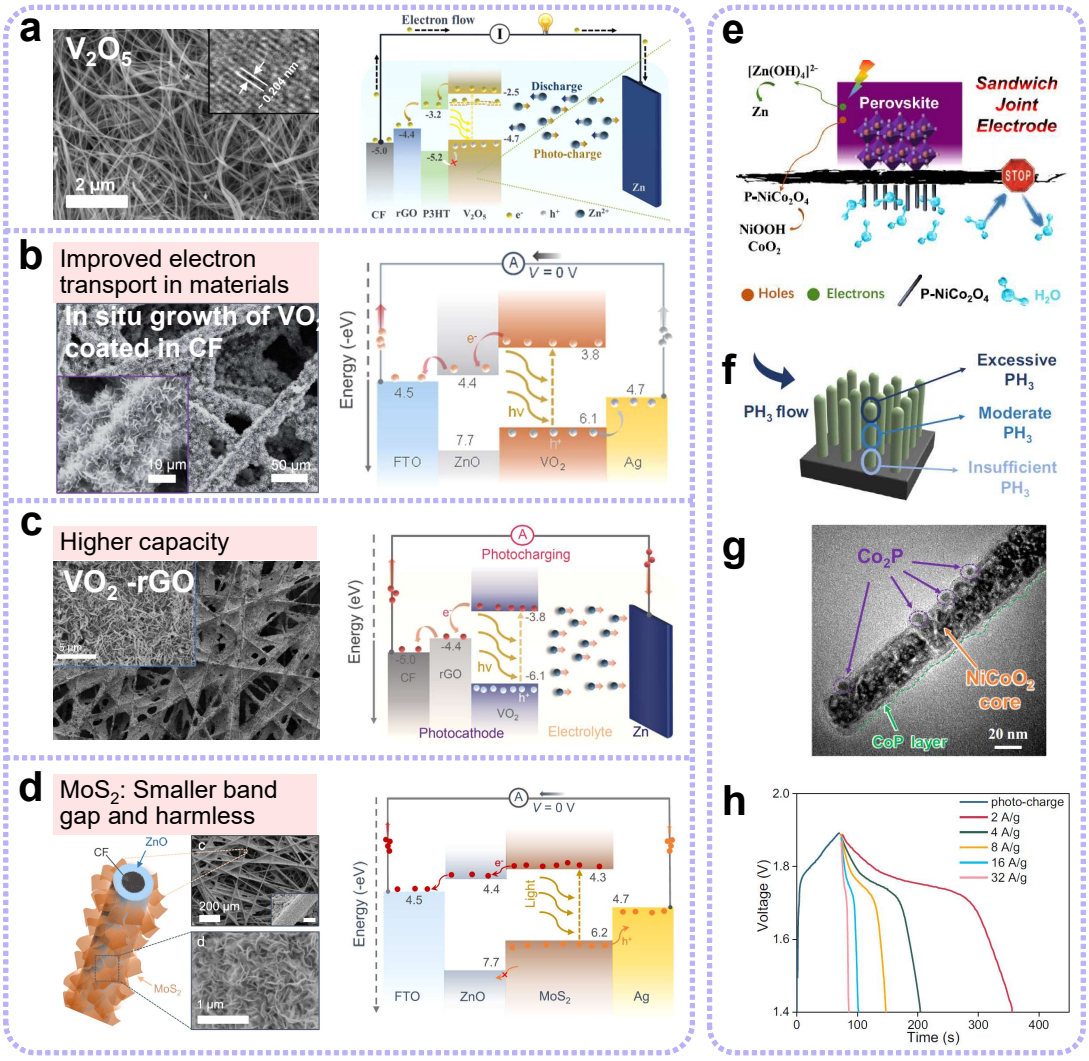

Figure 9. Examples of photo-assisted ZIBs. SEM images and work mechanisms of (a) an (FTO)/rGO/P_3HT/V_2O_5/Ag photoelectrode, (b) a VO_2/ZnO/CF photocathode, (c) an FTO/rGO/VO_2/Ag photoelectrode, and (d) a MoS_2/ZnO/CF photocathode in the ZIBs.

Reproduced with permission.[21] Copyright 2020, Royal Society of Chemistry. Reproduced with permission.[101] Copyright 2021, Royal Society of Chemistry. Reproduced with permission.[102] Copyright 2021, Wiley-VCH. (d) MoS_2/ZnO/CF photocathode. Reproduced with permission.[103] Copyright 2021, American Chemical Society. Schematic of (e) the integrated solar rechargeable ZIB and (f) phosphating process of the P-$NiCo_2O_4$ nanoarray. (g) HRTEM image of the Co_2P-CoP-$NiCoO_2$ nanoarray. (h) The discharge curves of the device after photo charging at different current densities. Reproduced with permission.[104] Copyright 2022, Springer Nature.

In recent years, rechargeable zinc-oxygen (Zn-O_2) batteries appear to be more attractive that other ones as energy storage devices for our society, due to their environmental benefits, high volumetric energy density, and renewable materials. The working principle of a Zn-O_2 battery is based on the reversible reaction of $2Zn + O_2 \leftrightarrow 2ZnO$, of which the theoretical equilibrium voltage is 1.64 V.[105–107] However, most of the reported Zn-air or Zn-O_2 batteries have actual discharge voltages lower than 1.2 V and the charge voltages higher than 2.0 V. The main reasons behind include the slow oxygen reduction reaction (ORR) and oxygen evolution (OER) reaction at the cathode, passivation and dendrite growth at the zinc cathode. To overcome such challenges, various strategies have been tried, such as the introduction of high-activity electrocatalysts, electrode protection, and electrolyte optimization. However, these Zn-air or Zn-O_2 batteries still have large charge/discharge voltage difference, ending with their low energy efficiencies.[107] Among newly developed strategies, the attempts to directly convert or store light energy in rechargeable batteries appear promising, although the challenges of how to achieve simultaneous conversion of light energy to electrical and chemical energy in the Zn-O_2 batteries have to be overcome. Namely, working mechanisms of such light-assisted zinc-air or Zn-O_2 batteries are poorly understood. One photo-assisted device example was constructed using a ZnS/CdSe/CdS/TiO_2/FTO photoanode in a zinc-air cell.[108] When compared to its charging in the dark, its charging under light illumination produced a gain of roughly 1.5 V. Following this work, they further improved the electrochemical performance of the light-

assisted Zn-O_2 battery, which had a voltage of up to 2 V **(Figure 10a)**[109]. The photoanode of the CdS/TiO_2 and a cathode of a Zn foil were applied to construct a light-assisted Zn-O_2 battery. A heterojunction array allows for efficient charge separation and collection, leading to improved energy conversion efficiency. An innovative photoelectrode was thus constructed by use of a unique step-scheme (S-scheme) heterojunction array (C_4N@TiO_2NR), which was obtained through in situ growth of *n*-type C_4N on aligned TiO_2 nanorods.[32] Due to this unique heterojunction structure, the appropriate staggered energy band is arranged. The built-in electric field induced significant photocurrent response and effective redox capability. Using C_4N@TiO_2NR as a photoelectrode of an acid-base/Zn-air hybrid cell, the device achieved a remarkably improve the electrochemical performance and accelerated kinetics of oxygen precipitation. Even at a small current density (e.g., 0.1 mA cm^{-2}), it realized a remarkable charge discharge voltage (0.43/2.02 V). When the current density increased to 10 mA cm^{-2}, it still exhibited an impressive charge/discharge voltage of 0.87/1.86 V. In addition to metal compounds, some organic polymers have been used in light-assisted Zn-O_2 batteries. For example, a Zn-O_2 battery was combined with a polymer semiconductor - polytrithiophene (pTTh) - as the cathode electrode of a Zn-O_2 battery **(Figure 10c)**.[110] This device directly converted energy into electricity for storage once light was harvested. Under light illumination, the photoelectrons generated in pTTh reduced oxygen to HO_2^-, while the anode of zinc metal was oxidized to ZnO. The discharge voltage of this photo-assisted zinc-air battery was dramatically raised to 1.78V without degrading over the course of 64 h of the discharging/charging cycles at a current density of 0.1 mA cm^{-2}, which translated to an improvement in energy density of 29.0% when compared to 1.38 V for a Zn-O_2 battery constructed using the cutting-edge Pt/C catalyst. In another study, poly(1,4-bis(2-thienyl) benzene (PDTB) and titanium dioxide (TiO_2) semiconductors were *in situ* loaded on carbon fibers as positive catalysts for the construction of Zn-O_2 batteries **(Figure 10d)**.[111] They were used for photoexcitation of the ORR and OER, respectively. Consequently, a circuit was formed with the porous zinc negative electrode during the discharging and charging processes, respectively. During the discharging process, the PDTB electrode was illuminated, and the

excited photoelectrons entered the conduction band of PDTB and injected into the molecular orbitals of O_2, thus promoting the ORR and raising the discharge voltage of the Zn-O_2 battery. During the charging process, the TiO_2 electrode was illuminated and strong oxidation holes were formed in the valence band and drove the OER under the action of the applied voltage. The generated photoelectrons were transferred to the negative electrode through the external circuit and reduced ZnO to Zn, in turn reduced the charging voltage of the cell. This sandwich Zn-O_2 cell structure ensured the simultaneous utilization of light energy during both discharging and charging processes. This Zn-O_2 battery possessed an intrinsically different reaction scheme for the simultaneous conversion of chemical and photo energy into electric energy. Therefore, it was believed to open a new pathway for the utilization of solar energy. Metal-based batteries are currently the most developed secondary energy storage devices, while their integration into light-assisted devices remains scarce. The future research activities should concentrate on the enhancement of their energy storage efficiencies and energy densities with aid of photo assisted devices. The development of photo self-recharge batteries has not been reported up to now. In most devices, the testing conditions of the devices are different, for example the wavelength range and the power density of the light source (e.g., a Xe lamp). In addition, there lacks the studies on the principles of the photo-assisted phases of these devices.

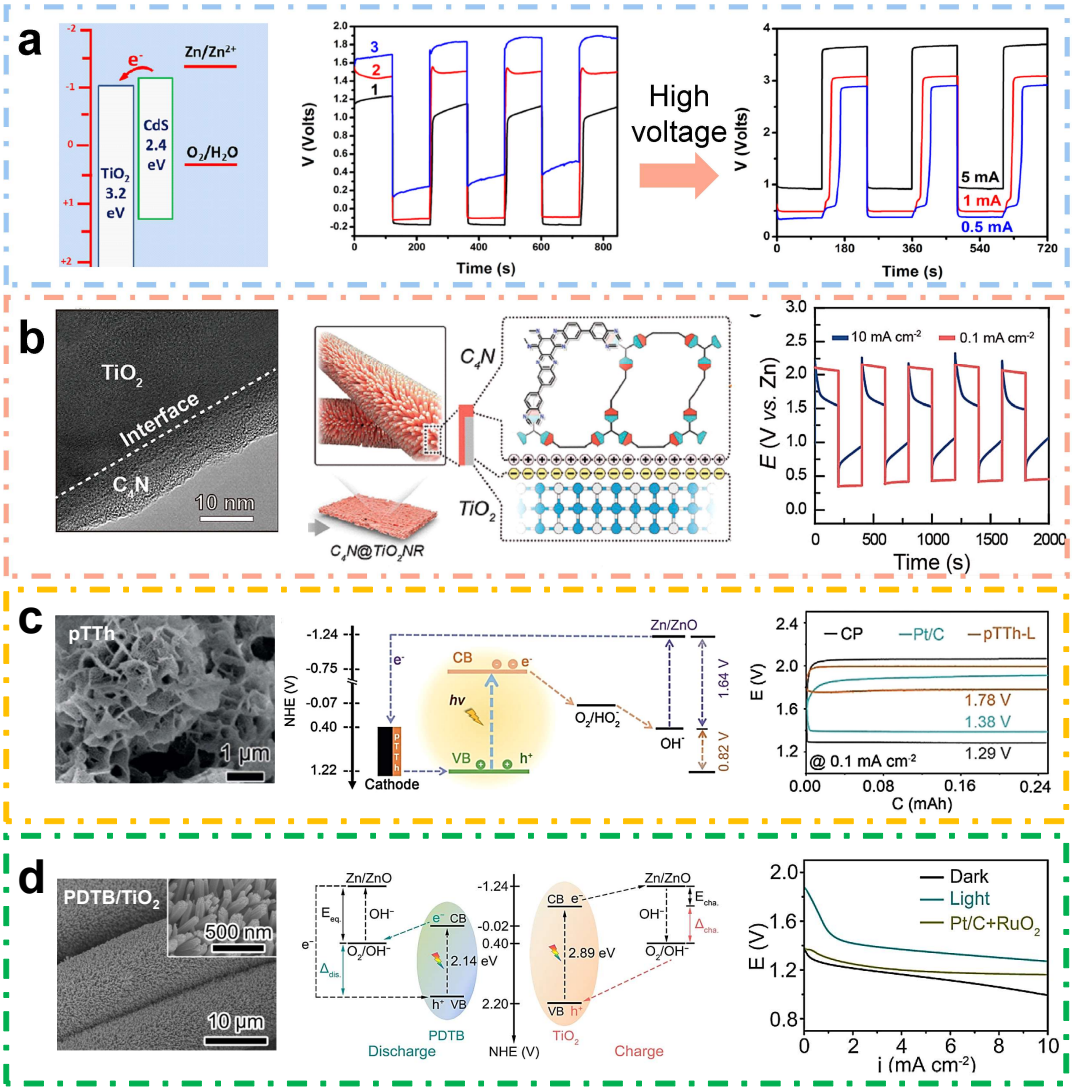

Figure 10. Examples of photo-assisted Zn-O_2 batteries. (a) Design and electrochemical performance of a photo-assisted Zn-O_2 battery with a high voltage. Reproduced with permission.[108,109] Copyright 2020, Elsevier. (b) TEM image and illustration of C_4N@TiO_2NR and the GCD curves of the device with light at different current densities (0.1, 10 mA cm^{-2}). Reproduced with permission.[32] Copyright 2020, Royal Society of Chemistry. SEM images of (c) polytrithiophene (pTTh) and (d) the mixture of poly(1,4-di(2-thienyl))benzene with TiO_2 as well as their work mechanisms and electrochemical performance as photo activated electrodes in photo-assisted Zn-O_2 batteries. Reproduced with permission.[110] Copyright 2019, Wiley-VCH. (d) poly(1,4-di(2-thienyl))benzene and TiO_2. Reproduced with permission.[111] Copyright 2020, Wiley-VCH.

3.4 Photo-assisted flow batteries

The energy storage principle of a flow battery is to realize the conversion of electric energy and chemical energy through redox reactions of active substances in the positive and negative electrolytes.[112,113] This battery can be repeatedly charged and discharged. Obviously, it owns different working principles from a traditional secondary battery. A flow battery is generally composed of a battery stack, a positive electrolyte, and a negative electrolyte. The battery stack mainly includes a positive electrode, negative electrode, and diaphragm. Depending on the active materials that are selected for the positive and negative electrodes, flow batteries can be classified as all-vanadium, zinc/bromine, zinc/chlorine, iron/chromium, and vanadium/polyhalide ones. Compared with Li metal batteries, Zn metal batteries, and other secondary batteries, flow batteries have the unique advantages, covering the independent design of power and capacity, suitability for large-scale energy storage, long service life (namely, up to 15000 cycles, the life span of 10-20 years), large energy storage capacity (namely, in the range of 100 kWh-1000 MWh), recycling possibilities of main materials, environmental friendless, and high energy efficiencies (namely, ＞80%). Moreover, it remains reversible charging/discharging performance. It can be deeply discharged without battery damage. Therefore, the flow battery, a new type of battery is very suitable as a storage device for renewable energy sources, such as wind and solar energy. It is thus expected to have a wide range of applications.

Once solar energy is directly converted to electricity and further stored in a flow battery, it will make the storage of renewable energy even easy and efficient. In this context, a solar rechargeable flow cell has been designed by combining a dual-silicon photoelectrochemical cell with a quinone/bromine redox flow battery.[114] Silicon-based photoanode and photocathode have an efficient utilization of solar energy thanks to the broad-spectrum absorption feature. As well as the fast reaction kinetics and excellent electrochemical reversibility of quinones, they can be used as energy storage active materials. An *in-situ* integrated system of solar energy-chemical energy-electrical energy triple conversion was then constructed. This system converted intermittent, low-energy-density solar energy into directly available continuous

electrical energy. Taking the AQDS/Br_2 liquid flow battery as an example, the constructed Solar rechargeable flow cell (SRFC) device charged itself under sunlight irradiation. Its energy utilization efficiency of photo-chemical conversion was as high as 5.9%. The initial discharge voltage of this battery after the charging was more than 0.8 V. The conversion rate of light energy in the whole photo charging/discharging process was more than 3.0%, the highest value reported for the same type of devices up to now. This device showed good stability during the charging/discharging cycles. Using inexpensive, ecologically friendly components, the first solar aqueous alkaline redox flow battery was designed **(Figure 11a)**.[115] The electrolytes had a typical cell potential of 0.74 V, which was composed of redox couples of ferrocyanide and anthraquinone-2,7-disulphonate in a sodium hydroxide solution. The ferrocyanide/hematite junction was used to illustrate photovoltage enhancement techniques. A layer of conductive polyaniline polymer was grown by an annealing procedure on the electrode surface to reduce electron-hole recombination. Another highly efficient solar flow battery has been shown in 2018.[116] Through a new type of integration, a record solar-to-output electricity efficiency of 14.1% was reached **(Figure 11b)**. Such solar flow batteries might be set up to carry out all necessary tasks, from collecting solar energy to redistributing power, without the influence of an outside source. For the formation of efficient solar flow batteries, tandem III-V photoelectrodes were paired with high-cell-voltage redox flow batteries in that they feature high efficiencies and high photovoltages. After careful design of the architecture in the flow fields, effective usage of solar energy and electrify off-grid homes were proved to be doable.

In addition to the optimization of the integration of electrodes and equipment, the electrolyte design of solar flow batteries was found to be important. In this regard, a silicon-based solar flow battery was designed with a neutral pH aqueous electrolyte,[117] which had strong organic redox couplings and reasonably priced photoelectrodes. This solar flow battery (SFB) device exhibited a very high-capacity utilization efficiency (above 80%). It was stably cycled over 200 h at a current density of 5 mA cm^{-2}. Such performance surpassed that of all previous systems, mainly due to the outstanding stability of both photoelectrodes and electrolytes. The device further achieved a significant increase of solar output efficiency up to 5.4% when single-

junction silicon photovoltaic electrodes were applied. The design concept to increase energy efficiency and prolong the device lifetime of such light-assisted flow cell was hoped to make them be competitive for off-grid applications. In recent years, some progress has been made in the field of light-assisted rechargeable flow batteries. To achieve superior performance and facilitate their early integration into practical applications, it is still crucial to develop additional redox couples that possess high solubility, fast kinetics, and excellent stability.

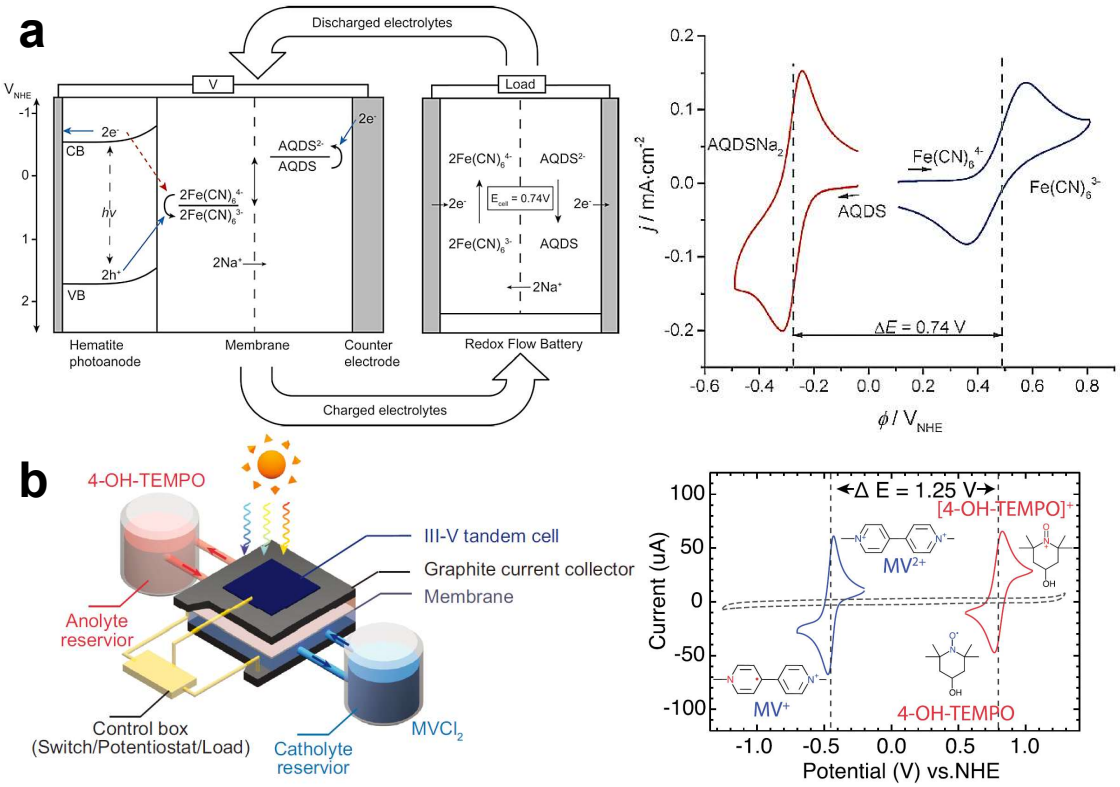

Figure 11. Example of photo-assisted flow batteries: Schematic representation and CVs of solar flow batteries (a) using a hematite photoanode and the redox pairs of ferrocyanide/AQDS and (b) using an III-V tandem photoelectrode and the redox couples of 4-OH-TEMPO/$MVCl_2$. Reproduced with permission.[115] Copyright 2016, Wiley-VCH. Reproduced with permission.[116] Copyright 2018, Cell Press.

3.5 Other photo-assisted batteries

In addition to lithium and zinc batteries, sodium and potassium batteries are of great significance as highly promising devices for energy storage. For example, sodium is abundantly

available on our earth. Sodium-ion batteries (SIBs) can be operated at room temperature, surpassing LIBs. A sodium metal has both a very high mass-to-capacity and a low reduction potential. It is thus considered an ideal cathode material for rechargeable batteries.[118] Meanwhile, sodium metal is desirable to create components for effective solar energy conversion and storage, because of its appealing qualities. For example, a saltwater battery was integrated into a photo-assisted rechargeable metal sodium battery after the addition of a photoelectrode of the TiO_2 nanotube array (TNT).[119] This battery exhibited a charge voltage of around 5.1 V in the dark. Using this solar saltwater battery, an energy efficiency of as high as 94% was achieved with a fast fall of the charge voltage down to 2.65 V under light illumination. In contrast, the use of heated carbon felt as the cathode in a seawater cell only produced the charge and discharge voltages of ~3.8 and ~2.9 V, respectively. The resultant energy efficiency was only ~76%. Note that the energy efficiency of the device equipped with a TNT photoelectrode was further increased under light illumination.

3.6 Photo-assisted flexible devices

With the rapid development of technology, various flexible portable and wearable electronic devices are highly demanded and already integrated into our daily lives. Meanwhile, the miniaturization of these smart devices (e.g., smart skin, implantable sensors, smart clothing) has been becoming increasingly important. In this context, micro-flexible energy storage devices are of the greatest importance since they can maintain good wear comfort and electrochemical stability of smart devices under various deformation states.[120,121] Moreover, smart devices face high energy consumption, resulting in the need of frequent charging inconvenience. Furthermore, these devices are often folded, squeezed, likely to bring safety risks. A flexible self-charging system that can directly obtain energy from the environment and simultaneously charge the energy storage devices but without external power sources is extremely attractive. In past years, different devices have been designed and developed, mainly including planar and fiber based flexible ones.

3.6.1 Planar flexible devices

A hierarchical porous and free-standing In_2S_3@CNT/SS (ICS) photocathode has been utilized to fabricate a flexible photo-assisted Li-CO_2 battery **(Figure 12a)**.[22] This Li-CO_2 battery owned a record-high discharge voltage of 3.14 V, above the thermodynamic limit of 2.80 V. It possessed an ultra-low charge voltage of 3.20 V. Moreover, it yielded a round trip efficiency of 98.1%, the highest value recorded so far. Such outstanding electrochemical performance was attributed to the multi-layer and porous structure of the ICS photocathode. In more detail, this structure facilitated the fast transport of electrons and holes inside the material. These novel reaction schemes provide both light/electricity energy conversion and storage inside a Li-CO_2 cell. The remarkable flexibility of the Li-CO_2 pouch battery was considered to be hopeful to expand the use of solar energy and batteries, including portable devices. A light-driven flexible anode for a Li-O_2 battery was prepared by combining electrostatic spinning with chemical deposition, namely by directly mixing WSe_2 with carbon nanotubes **(Figure 12b)**.[122] This electrode exhibited a capacity of 57.17 mAh cm^{-1} in the dark. Once it was illuminated, its capacity was three times increased, while the discharge/charge voltage gap was reduced to 0.49 V. The exceptional battery performance was attributed to the reversible Li_2O_2 conversion that was catalyzed by WSe_2 as well as to the photo-enhanced electrochemical microenvironment at both the cathode and anode.

In 2018 one ultrathin flexible all-solid-state light-assisted SC has been designed **(Figure 12c)**.[123] The bi-polar TNT was adopted as a substrate to integrate the SC with a solar cell to form a sandwich structure, where direct transfer of electrons and holes from solar cell to the SCs was observed. When the simulated sunlight illuminated this light-assisted SC, its voltage immediately rose to 0.63 V within 30 s. Moreover, it exhibited a PV conversion efficiency of 4.9% and the storage efficiency of up to 80%. Its response was fast and its cycling capability was stable. To meet the applicable requirements for larger output voltages, these optoelectronic SCs were woven into a "bamboo slip" structure that can be folded and bent, exhibiting excellent flexibility. For example, an ultra-thin photo-charging system with a whole thickness below 50 μm was designed and produced **(Figure 12d)**.[124] It contained 40-μm thick carbon

nanotube/polymer-based SCs and 3-μm thick organic photovoltaics. Its total efficiency was approximately 6%. This efficiency was improved by approximately 15% when compared to previous reports, but the device only had a 1/8 thickness. This device also exhibited excellent cycling performance. Its retention rate was more than 96% of its initial value even after 100 charging/discharging cycles at a current density of 3 mA cm^{-2}. Its mechanical stability was high, together with a capacity retention rate of 94.66% after 5000 bending cycles. This ultra-thin device provided fresh perspectives on the design of powerful flexible and wearable devices.

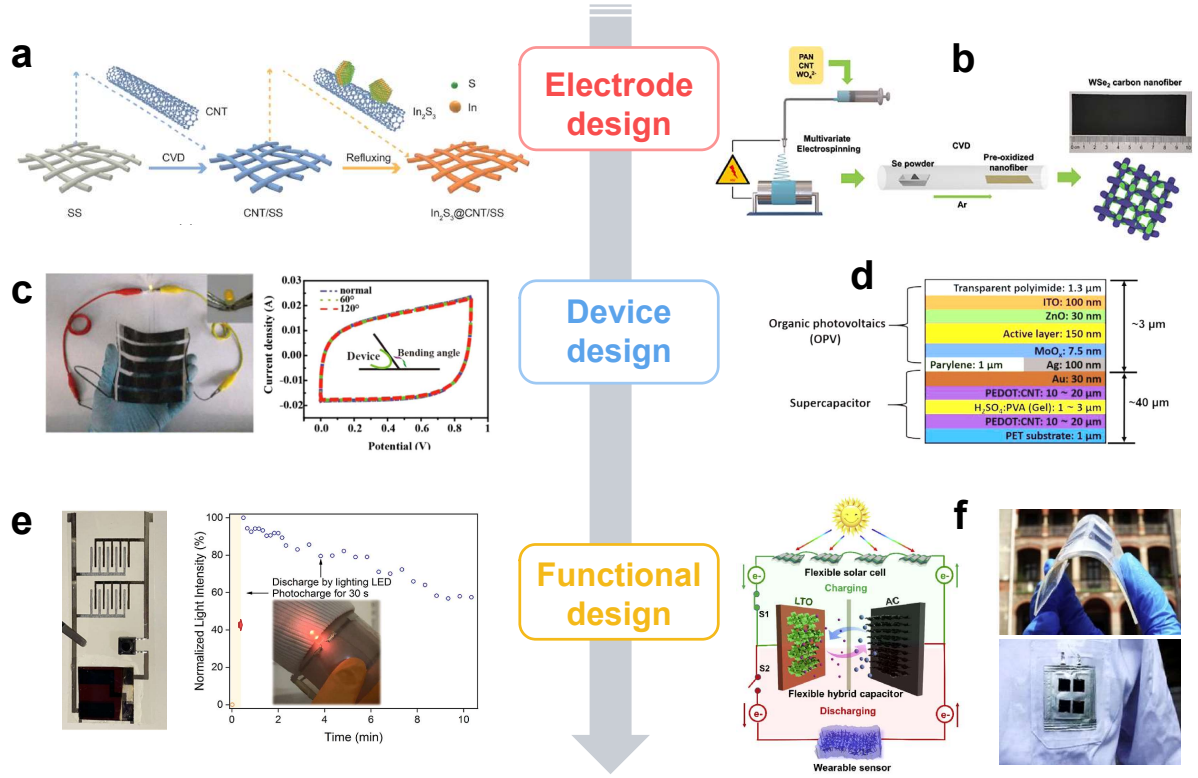

Figure 12. Examples of planar photo-assisted energy storage devices. The design and preparation scheme of (a) In_2S_3@CNT/SS and (b) WSe_2 carbon nanofibers. Reproduced with permission.[22] Copyright 2020, Wiley-VCH. and (b) WSe_2 carbon nanofibers. Reproduced with permission.[122] Copyright 2022, Elsevier. (c) Optical image of a flexible photo-SC that powered a commercial light under bending conditions as well as the CVs of this device at different bending angles. Reproduced with permission.[123] Copyright 2018, Elsevier. (d) Schematic illustration of a top-down ultra-thin photo-charging integrated device. Reproduced with permission.[124] Copyright 2020, Wiley-VCH. (e) Optical image and performance of a photo-

rechargeable zinc-ion micro-battery. Reproduced with permission.[125] Copyright 2022, Elsevier. (f) Schematic illustration and photographs of a flexible photo-rechargeable self-powered wearable strain sensor. Reproduced with permission.[17] Copyright 2019, Elsevier.

In the aspect of device miniaturization, stable and ultrafast quasi-solid-state Zn-MnO_2 micro batteries (ZMB) have been combined with flexible perovskite solar cells by use of inkjet printing and electrodeposition methods **(Figure 12e)**.[125] To stabilize the battery structure and improve the electrochemical performance of such a device, a Ni protective layer was initially added to the ZMB. Such a ZMB showed excellent electrochemical performance. Its power density was 55 W cm^{-3} and its volumetric energy density was 148 mWh cm^{-3}. The integrated flexible perovskite solar cell (FPSC) exhibited good photovoltaic performance, having adequate energy to power ZMBs and build a self-charging system. It was capable of providing energy independently in wearable electronics with small form factors. The combined systems performed ultrafast photo-charging within 30 s. It had enough energy to operate or function additional electronics (e.g., an LED light, a pressure sensor) for tens of minutes. This prototype was thus proposed for the next-generation, flexible, tiny photo-rechargeable devices. In another example, a flexible photo-rechargeable lithium-ion capacitor combined energy harvesting and storage for self-powering wearable strain sensors for the first time **(Figure 12f)**.[17] With a discharge current density of 0.1 A g^{-1}, this adaptable and photo-rechargeable lithium-ion capacitor achieved a high output voltage of 3 V and an increased performance of 8.41%. Even at a high current density of 1 A g^{-1}, it still produced an astounding overall efficiency of more than 6%, outperforming cutting-edge photo-charging power sources. This self-powered strain sensor exhibited the ability to record physiological signals accurately and continuously without the need for external power connections. This was accomplished using the synergy of energy harvesting, storage, and use inside a single intelligent system. It was envisaged that this multi-field-coupled, function-integrated platform will provide important advantages for useful self-powered wearable electronics.

3.6.2 Fiber flexible devices

Although planar flexible devices are flexible to a certain extent, they are still inadequate in terms of flexibility, device integration, and wear ability. It is thus important to develop flexible energy storage devices that can maintain good wearing comfort and electrochemical stability under various deformation conditions and meanwhile have high integration and wear ability. A flexible fiber device is one of the best options, due to its unique wire-like structure, small size, and light mass.[126–128] For example, it can be easily woven into various fabrics for energy supply. It thus meets the requirements of miniaturization, integration, and wear resistance of flexible energy storage devices, although the design and integration process are somehow difficult. The current strategy to form such photo-assisted fiber cells is to integrate solar cells with energy storage devices simply through wires. For example, a power-fiber device was fabricated by the combination of a dye-sensitized solar cell (DSSC) and a twisted-fiber SC **(Figure 13a)**.[129] The electrodes of the device were made of a stainless-steel wire that was deposited with polyaniline. They were used together for both fiber DSSC and fiber SC. Such a flexible device had an overall energy conversion efficiency of 2.1%. Since the powered fiber was tiny, flexible, wearable, and less costly, this device was ideal for some specialized applications. It was expected to be capable of merging with fabrics in contrast to conventional integrated power systems. On the contrary to traditional integrated power systems, the integrated power fiber was lightweight, flexible, inexpensive, and suitable for different special applications. Later, a 31 cm-long flexible fiber dye-sensitized solar cell[130] was combined with a zinc bromide cell **(Figure 13b)**. Using this device, an overall conversion rate of 3.42% was achieved. The entire process of preparation was simple to be managed and thus appropriate for mass manufacturing **(Figure 13c)**. However, during the bending of such flexible devices, two twisted fiber electrodes came apart. The liquid electrolyte of the solar cell was diffused into its SC component. It was still stated that this study might lead the way for adaptable, lightweight, and effective power sources.

Another coaxial fiber photo SC was designed by integrating the dye-sensitized solar cells and SCs.[121] The inner electrode consisted of metallic titanium as a substrate where a vertically aligned layer of titanium dioxide was deposited. The outer electrode was coated with a multi-

walled carbon nanotube film **(Figure 13d)**. The photoelectric conversion and energy storage efficiency of this cell were 2.73% and 75.7%, respectively. This flexible fiber device was then woven into varieties textiles. It maintained good performance when bent or squeezed. Polymer solar cells were safer because they do not require a liquid electrolyte. In this aspect, an all-solid-state flexible "energy fiber" was designed and produced by combining a polymer solar cell with a fiber SC featuring a coaxial structure **(Figure 13e)**.[132] This device directly converted solar energy into electrical energy for storage. Since the photoelectric conversion component was radially comparable to an effective planar polymer solar cell, the produced charges were quickly transferred and separated to create large photocurrents. The coaxial configuration for the electrochemical storage component also favored quick charge transmission since it had a substantially bigger effective contact area than the previously studied twisted structure of two fiber electrodes with high electrical resistances **(Figure 13f)**.

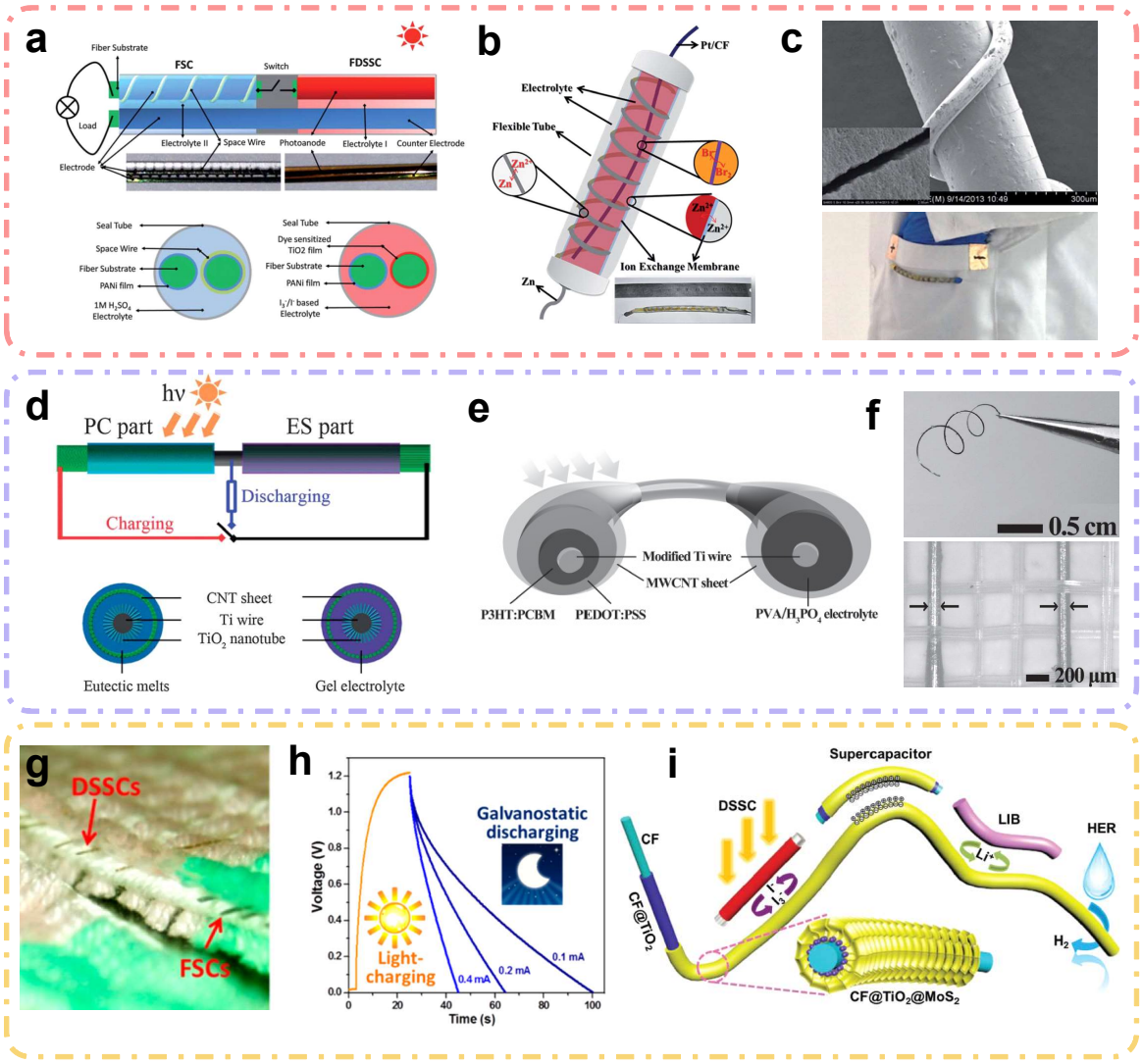

Figure 13. Examples of fibrous photo-assisted energy storage devices. (a,b) Structural schematic and photograph of a photo-assisted energy storage device twist incorporated using a dye sensitized solar cell and an SC. (c) SEM image of a flexible photoanode after bending 200 times and a photo of a flexible device that was integrated into the cloth. Reproduced with permission.[129,130] Copyright 2013, 2015, Royal Society of Chemistry. (d,e) Schematic illustration of a photo-assisted energy storage device that coaxially integrated a PV cell conversion and an SC. (f) Photographs of the flexibility and weave ability of the device. Reproduced with permission.[131,132] Copyright 2014, Royal Society of Chemistry. Copyright 2014, Wiley-VCH. (g) Photograph of a fiber device fabricated and tailored into the cloth. (h) The discharging curves of the device after photo illumination. Reproduced with permission.[133] Copyright 2016, American Chemical Society. (i) Schematic illustration of a coaxial fibrous MoS_2-based all-purpose fibrous electrode and its various applications for energy harvesting and storage. Reproduced with permission.[134] Copyright 2017, Wiley-VCH.

An all-solid tailorable energy textile was also introduced **(Figure 13g)**.[133] This device was prepared directly using textile to integrate solar energy harvesting and storage. The process enabled the creation of fashionable smart energy garments for a wearable self-powering system with improved user experience and greater flexibility for the fashion design. While it still allowed the multifunctional textile to be tailored into any intended shape without compromising its functionality. Its large-scale production and reparation were thus stated to be possible simply by removing the damaged component. In another all-solid dye-sensitized solar cell, textile was employed as the solar energy harvesting module, while a fiber SC was used as the energy storage module. By using solar energy that was generated on its own, the textile sample was fully charged to 1.2 V within 17 s. The entire discharge at a current density of 0.1 mA cm^{-2} was done within 78 s **(Figure 13h)**. Since such a device was tailorable, ultrafast charged, and owned ultrahigh bending resistance, it enabled the creation of fashionable smart energy clothing with improved user experience as well as great flexibility for fashion design. In another report, a multifunctional fibrous electrode was designed **(Figure 13i)**[134] to realize the self-powered and

direct conversion of light energy into electricity. It was used for fibrous LIBs and electrocatalytic hydrogen evolution reactions. Carbon fibers were used as the electrode substrate. After a layer of TiO_2 nanoparticles was coated on its surface, a MoS_2 layer with a nanometer thickness was grown. This DSSC device showed a conversion efficiency of as high as 9.5%. Such a high efficiency was mainly due to the synergistic effect of the high electrochemical activity of MoS_2 and the high conductivity of carbon fibers. Additionally, a fibrous DSSC and a fibrous SC were combined to create a self-powering energy fiber. It was charged within 7 s under AM1.5G solar illumination. Its overall photochemical-electricity energy conversion efficiency was as high as 1.8%. The development of such flexible light-assisted devices is expected to be a promising solution to realize device miniaturization and integration as well as to maintain wear resistance of flexible energy storage devices. This section provides a summary of the advancements in light-assisted flexible devices. However, most of the reported studies only focused on individual photoelectric conversion (e.g., solar cells) and energy storage devices (e.g., SCs, Li-ion batteries), rather than integrated ones. There have been no significant breakthroughs in the research of light-driven fiber-like flexible energy storage devices in recent years, which means that we face significant challenges and opportunities. It is hoped that more researchers will address these difficulties in order to achieve an early breakthrough. Additionally, flexible devices are predominantly utilized in wearable and irregularly shaped applications, necessitating targeted designs that incorporate features like self-healing capabilities, resistance to random shearing, and compatibility with irregular shapes. Consequently, there is an urgent requirement to conduct research aimed at developing improved flexible devices with dual functionality.

3.6.3 solid electrolyte

In the quest for innovative solutions to address safety concerns associated with liquid electrolyte batteries, solid-state electrolytes have emerged as a promising alternative, thanks to their superior stability under different photo, thermal, and chemical conditions.[135,136] Moreover, the devices utilizing solid electrolytes offer greater design flexibility compared to those using liquid

electrolytes, making them adaptable to various shapes. Given the increasing popularity of flexible wearable devices, the research on solid-state electrolytes has become imperative. Solid-state electrolytes thus hold particular significance in light-assisted energy storage devices. The introduction of light in energy storage systems brings several advantages, such as enhanced energy output and reduced charge/discharge potential of electrode materials.[137] However, certain inevitable challenges exist. For instance, the light exposure or continuous light illumination might lead to electrolyte breakdown, electrolyte corrosion of photosensitive materials, and temperature elevation. Unfortunately, seldom reports focused on the electrolytes used for light-driven energy storage devices, particularly in the realm of solid-state electrolytes. A tactile, UV- and solar-light multi-sensing smart all-solid-state Zn–air battery (SRZAB) with high performance was designed and reported.[138] The electrode of this device was constructed by multi-scale conjugated block-copolymer with carbon nanotube (CNT)–polyurethane foam. The mixed gel of PVA/PEO/KOH was used as the solid electrolyte. This unique electrode structure triggered effective electronic and ionic transport and interfacial redox reactions. The addition of solid electrolytes gave the SRZAB good mechanical properties, enhanced mass transport, and improved thermal effect. Its increased electrochemical performance resulted from reduced charging voltages, reduced energy consumption, and meanwhile accelerated response rates of ORR and OER under UV light irradiation. This SRZAB featured an energy efficiency of 69%, an energy density of 1272 Wh L_{Zn}^{-1}, and good cycling stability. In addition, it showed good flexibility and stress resistance, and maintained good electromechanical performance even after 90% compressive strain. This work is believed to serves as the inspiration of next-generation smart electronics and optoelectronics.

Solar energy inherently undergoes both photovoltaic and photothermal conversions, where the latter is often overlooked. However, the potential of harnessing the sun's inherent photothermal effect has been recognized and utilized to design self-heating batteries.[50,51,139] This approach holds the promise of achieving significant advancements in the field of low-temperature batteries. A solar driven all-solid-state lithium-air battery with plasmonic air cathode and $Li_{1.5}Al_{0.5}Ge_{1.5}P_3O_{12}$ (LAGP) solid-state electrolyte has been proposed.[139] It captured sunlight

efficiently and converted it into heat, leading to improved charge transfer and storage at ultra-low temperatures. The incorporation of a plasmonic air electrode that consisted of CNT and Ru nanostructures improved remarkably the absorption efficiency (> 95%) of the solar spectra. When exposed to solar light, the electrode enhanced charge storage and transmission within the electrolyte and electrode materials. The resistances of the lithium-air battery with the plasmonic air electrode were then significantly reduced, even at extremely low temperatures (e.g., −73 °C). Consequently, this battery demonstrated an exceptional cycle life of over 50 cycles at room temperature and even stably cycle for 15 cycles at −73 °C with a capacity limitation of 1000 mA h g^{-1} at a current density of 400 mA g^{-1}. By leveraging the photothermal effect, this battery overcame the challenges posed by low temperatures. Meanwhile, it potentially achieved breakthroughs in its performance and efficiency.

Similarly, porous Au@TiO_2/LAGP framework and a bilayer LAGP electrolyte were employed to construct an all-solid-state light-assisted Li-CO_2 battery.[50] The Au@TiO_2 composite exhibited the capability to absorb the entire spectrum of solar energy, enabling the conversion of light into both heat and electricity. Its combination with LAGP-based framework further lowered the kinetic barriers of the CO_2 reduction reaction and hydrogen evolution reaction at an ultrawide temperature window. The bilayer LAGP structure maintained the structural stability of the electrode during photothermal and photoelectric effects, facilitating rapid transfer of light, heat and Li^+ ions. Remarkably, this battery offered an exceptionally high discharge voltage of 3.00 V and delivered a small polarization of 0.6 V even at a temperature as low as −73 °C, while maintaining a round-trip efficiency of 84.5%. These pioneer works inspired the rational use of the solar thermal and photovoltaic properties, as well as initialize ideas for large-scale energy supply in extremely cold regions. To further enhance the performance of metal-air batteries, a novel photo-assisted solid-state Li−O_2 battery has been further designed[51]. Unlike previously reported solid metal batteries, this device used a mixed ionic-electronic conductor based on metal-organic framework as both the cathode and the solid electrolyte. This mixed ionic-electronic conductor allowed effective improvement of interfacial charge-transfer kinetics compared to the previous separated electrolytes and electrodes. The

introduction of light further reduced energy barriers, accelerated reaction kinetics and enhanced related catalytic activity, resulting in increased electrochemical performance (e.g., a round-trip efficiency of > 90% and longer lifetime than 320 cycles).

In spite of these breakthroughs, the research field of solid-state electrolytes for photo-assisted batteries remains unexplored. It is therefore vital that additional effort and resources need to be invested in upcoming years. In this regard, high-performance solid-state electrolytes should be designed and synthesized. For example, solid polymers with high ionic conductivity and flexibility must be selected. The interfacial transport between the polymer and the electrodes needs to be optimized. The safety of the constructed device should be ensured. The clear address of these issues together with other different strategies (e.g., the use of nanocomposites or composite nanoelectrodes, interfacial engineering), the development of solid-state electrolytes for high-performance light-assisted batteries is expected.

4. Summary and perspectives

Light-assisted energy storage devices or photo-rechargeable integrated devices are generally made up of solar cells/photoelectrodes and electrochemical energy storage units (e.g., SCs and batteries). They have drawn attention on a global scale since they can directly convert harvested solar energy into stored electrochemical energy. Due to their exceptional benefits, such as high efficiencies, versatile applications, portability, and wearability, the design and manufacture of these sophisticated integrated devices for hybridizing solar energy harvest and storage processes have received extreme attention up to date. This review summarizes the most recent progress and achievements in various photo-assisted rechargeable devices, including light-driven rechargeable metal-ion batteries, metal-O_2 batteries, metal-CO_2 batteries, flow batteries, and SCs.

In spite of such progress and achievements, the field of light-assisted energy storage devices is still in its infancy. There are many challenges to be overcome. First, current materials are less selective and less compatible, which leads to lower photovoltaic conversion and increased resistivity of the integrated modules. The availability of redox couples for light-assisted energy

storage devices is quite limited. Poor compatibility between materials also affects the durability and stability of the devices. Second, combining energy conversion and storage in one device may lead to some reactions between the photosensitive material and the active electrode or electrolyte, resulting in low conversion efficiency and unstable device cycling. In most devices liquid electrolytes are employed, where leakage or evaporation potentially often occurs. In other words, the performance and function of the devices can be seriously affected. Third, the mechanisms of these light-assisted energy storage devices have not been fully revealed, although there have been some studies on their photoelectric conversion processes. This is due to the difficulties to observe structural changes during solar energy conversion and in the course of its *in situ* storage. This significantly hinders the further development of photo-assisted devices. Finally, there is a lack of standardized test protocols and long-term feasibility. There are no common test protocols to analyze the same benchmarks for different devices. For example, the overall efficiencies reported by newly manufactured devices do not follow any common procedures or test strategies.

In order to achieve high-performance photo-assisted energy storage devices and further enhance their practicality, the studies in the following aspects are suggested to be considered and conducted for the future development of photo-assisted energy storage devices (**Figure 14**).

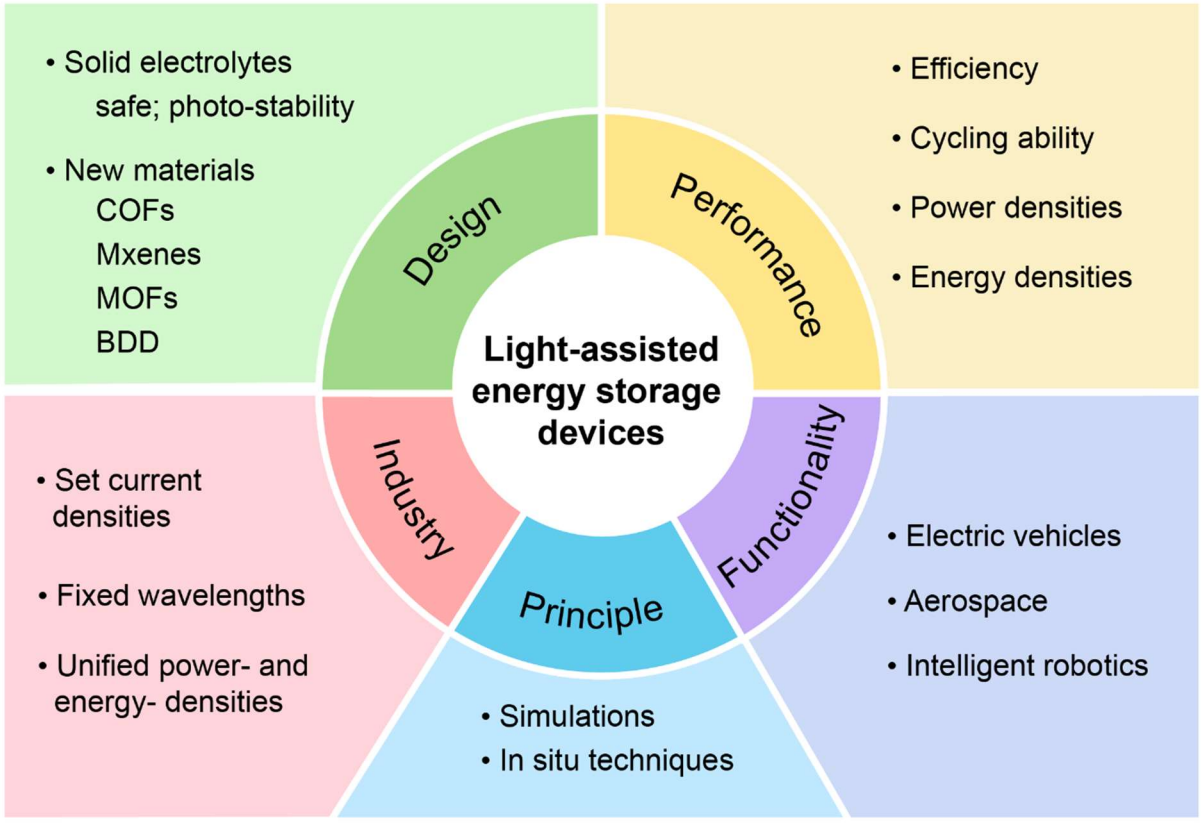

Figure 14. Future perspectives for the design and development of photo-assisted energy storage devices.

Working principles: Detailed mechanisms of these light-assisted energy storage devices have not yet been revealed. More advanced and *in situ* characterization techniques (e.g., *in situ* confocal photoluminescence, *in situ* Raman, *in situ* liquid phase transmission electron microscopy, *in situ* XRD, *in situ* FTIR, *in situ* synchrotron X-ray absorption spectroscopy) need to be developed and applied to achieve depth understanding of the photo-electron conversion and energy storage processes in the devices.

Design of new photo-activated material: more novel materials need to be designed, synthesized, and introduced into light integrated energy storage device systems for efficiency improvement. For example, single-atom catalysts have been proved to exhibit ultra-high catalytic activity for a variety of redox reactions.[140,141] If they are introduced into the DSSCs or LIBs, the overall performance of a hybrid system is expected to be significantly enhanced, due to optimized electrochemical reactions. Various quantum dots are also attractive for light-assisted energy

storage devices. This is because they can greatly increase the PV conversion efficiencies of solar cells as well as improve the rate capability of a PV cell.[142,143] Mxenes are also the alternatives for light-assisted energy storage devices since their high mobility as the main charge transport channels can significantly enhance electron transport.[144] In addition, some new composites or hybrids appear to be interesting for light-assisted energy storage devices, such as the composites of boron-doped diamond (BDD) and titanium dioxide. Such composites have good stability, while a wide electrochemical window of BDD provides sufficient bias voltage to enhance the photochemical performance of the TiO_2 photocatalysts.[145,146] Porous metal-organic frameworks (MOFs) and covalent organic frameworks (COF) are known to be rich in their active sites.[147,148] Once they are introduced into the electrodes of light-assisted energy storage devices, it is expected that the rate capability and stability of the integrated devices are possibly significantly improved. In addition to them, there are a number of photochromic or photothermal materials that shall be considered for the design of more creative optoelectronic devices.

Development of solid electrolytes: In most reported solar cells or SCs or metal-ion/air cells, most electrolytes are organic or ionic liquid electrolytes. Such electrolytes become less stable and have a negative impact on photoactive and electrode materials under long-term light illumination. In this regard, the development of electrolytes with high photo-stability and electrochemical stability is essential for the overall stability of light-assisted energy storage devices. If the photo-assisted energy storage devices are assembled in wearable devices, they must be safe and stable enough. Solid electrolytes fit here better than liquid electrolytes since they offer better photo-thermal stability and safety.[149] When applied to flexible devices where repeated folding and squeezing may lead to liquid leakage, solid electrolytes are definitely safer. Solid electrolytes featuring high ionic conductivities at high temperatures are therefore required. Consequently, further performance improvement of these solid batteries is needed.

Design of functional photo-induced devices: For different types of light-assisted energy storage devices for unique applications that shall be designed considering. With their high-power densities and long cycle life, light-assisted SCs are well-suited for large-scale integrated energy

storage applications. They can effectively provide the total energy requirements for governments, businesses, or households. Wireless sensor networks and IoT devices are often widely distributed in various locations, far from power outlets. Therefore, light-assisted energy storage devices with high volume energy densities, such as light-assisted lithium-ion batteries, are expected to have their advantages. For industrial applications such as electric vehicles, aerospace, and intelligent robotics, light-assisted energy storage devices with higher energy densities and higher safety can be used. Furthermore, portable devices and wearable devices require a high degree of safety and comfort due to their contact with the body. In this regard, flexible light-assisted aqueous metal batteries are better suited. Additionally, self-heating light-assisted devices enable device operation in extremely cold regions through photothermal conversion. Studies in this area are inadequate and more efforts are required. In short, different designs of light-assisted energy storage devices are needed for specific application scenarios.

Establishment of industry standards: there is no uniformity regarding the specific conditions and requirements for testing. Current studies focus more on the novelty of material design and conversion efficiency. To test light-assisted energy storage devices at a fixed wavelength or a set current density, different standards, especially for practical applications need to be set up. A routine analysis roadmap is a must to effectively assess the performance of various light-assisted energy storage devices as well as to analyze their future development trend.

In summary, light-assisted energy storage devices open up a new way to better meet the growing energy demand in the future. They bring new inspiration for the development of some new green energy devices, such as solar rechargeable battery-based electric vehicles. They are promising and useful for renewable, portable, smart electronic devices if their advantage of miniaturization, portability and wearability can be further integrated. For sure, there are still very many challenges for light-assisted energy storage devices that have to be overcome and solved before their real movement towards commercialization and for industrial applications.

Acknowledgements

X. Dong thanks the China Scholarship Council (CSC) for the financial support (No.

202106250006). X. Chen thanks the China Scholarship Council (CSC) for the financial support (No. 202008420219). N. Yang thanks the financial support from the Deutsche Forschungsgemein-schaft (DFG, German Research Foundation) under the project of 457444676.

Conflict of Interest

The authors declare no conflict of interest.

Received: ((will be filled in by the editorial staff))

Revised: ((will be filled in by the editorial staff))

Published online: ((will be filled in by the editorial staff))

References

[1] P. Simon, Y. Gogotsi, B. Dunn, *Science* **2014**, *343*, 1210.

[2] P. Simon, Y. Gogotsi, *Nat. Mater.* **2020**, *19*, 1151.

[3] Polman, M. Knight, E. C. Garnett, B. Ehrler, W. C. Sinke, *Science* **2016**, *352*, 4424.

[4] P. K. Nayak, S. Mahesh, H. J. Snaith, D. Cahen, *Nat. Rev. Mater.* **2019**, *4*, 269.

[5] Y. Zhao, Y. Zhu, H.-W. Cheng, R. Zheng, D. Meng, Y. Yang, *Mater. Today Energy* **2021**, *22*, 100852.

[6] M. I. H. Ansari, A. Qurashi, M. K. Nazeeruddin, *J. Photochem. Photobiol. C Photochem. Rev.* **2018**, *35*, 1.

[7] J. Lv, J. Xie, A. G. A. Mohamed, X. Zhang, Y. Wang, *Chem. Soc. Rev.* **2022**, *51*, 1511.

[8] Z. Fang, X. Hu, D. Yu, *ChemPlusChem* **2020**, *85*, 600.

[9] Y. Zhong, X. Xia, W. Mai, J. Tu, H. J. Fan, *Adv. Mater. Technol.* **2017**, *2*, 1700182.

[10] D. Schmidt, M. D. Hager, U. S. Schubert, *Adv. Energy Mater.* **2016**, *6*, 1500369.

[11] A. Gouda, S. R. Bobbara, M. Reali, C. Santato, *J. Phys. D: Appl. Phys.* **2019**, *53*, 043003.

[12] G. Hodes, J. Manassen, D. Cahen, *Nature* **1976**, *261*, 403.

[13] C.-Y. Hsu, H.-W. Chen, K.-M. Lee, C.-W. Hu, K.-C. Ho, *J. Power Sources* **2010**, *195*, 6232.

[14] Hauch, A. Georg, U. O. Krašovec, B. Orel, *J. Electrochem. Soc.* **2002**, *149*, A1208.

[15] T. Miyasaka, T. N. Murakami, *Appl. Phys. Lett.* **2004**, *85*, 3932.

[16] M. Yu, X. Ren, L. Ma, Y. Wu, *Nat. Commun.* **2014**, *5*, 5111.

[17] C. Li, S. Cong, Z. Tian, Y. Song, L. Yu, C. Lu, Y. Shao, J. Li, G. Zou, M. H. Rümmeli, S. Dou, J. Sun, Z. Liu, *Nano Energy* **2019**, *60*, 247.

[18] X. Liu, Y. Yuan, J. Liu, B. Liu, X. Chen, J. Ding, X. Han, Y. Deng, C. Zhong, W. Hu, *Nat. Commun.* **2019**, *10*, 4767.

[19] Y. Man, Q. Hao, F. Chen, X. Chen, Y. Wang, T. Liu, F. Liu, N. Li, *ChemElectroChem* **2019**, *6*, 5872.

[20] B. D. Boruah, A. Mathieson, B. Wen, C. Jo, F. Deschler, M. De Volder, *Nano Lett.* **2020**, *20*, 5967.

[21] B. Boruah, A. Mathieson, B. Wen, S. Feldmann, W. M. Dose, M. D. Volder, *Energy Environ. Sci.* **2020**, *13*, 2414.

[22] D.-H. Guan, X.-X. Wang, M.-L. Li, F. Li, L.-J. Zheng, X.-L. Huang, J.-J. Xu, *Angew. Chem. Int. Ed.* **2020**, *59*, 19518.

[23] X. Liu, S. Tao, J. Zhang, Y. Zhu, R. Ma, J. Lu, *J. Mater. Chem. A* **2021**, *9*, 26061.

[24] R. Liu, Z. L. Wang, K. Fukuda, T. Someya, *Nat. Rev. Mater.* **2022**, *7*, 870.

[25]N.-F. Yan, X.-P. Gao, *Energy Environ. Mater.* **2021**, *0*, 1.

[26]K. Jost, G. Dion, Y. Gogotsi, *J. Mater. Chem. A* **2014**, *2*, 10776.

[27]D. Yu, Q. Qian, L. Wei, W. Jiang, K. Goh, J. Wei, J. Zhang, Y. Chen, *Chem. Soc. Rev.* **2015**, *44*, 647.

[28]X. Dong, J. Liang, H. Li, Z. Wu, L. Zhang, Y. Deng, H. Yu, Y. Tao, Q.-H. Yang, *Nano Energy* **2021**, *80*, 105523.

[29]P. Li, T. Shang, X. Dong, H. Li, Y. Tao, Q. Yang, *Small* **2021**, *17*, 2007548.

[30]H. Meng, S. Pang, G. Cui, *ChemSusChem* **2019**, *12*, 3431.

[31]J. Liu, M. Wang, Z. Tao, L. He, C. Guo, B. Liu, Z. Zhang, *Anal. Chim. Acta* **2023**, 341396.

[32]X. Wang, Y. Li, M. Yang, C. Liu, J. Li, D. Yu, *Adv. Funct. Mater.* **2022**, *32*, 2205518.

[33]N. Choudhary, C. Li, J. Moore, N. Nagaiah, L. Zhai, Y. Jung, J. Thomas, *Adv. Mater.* **2017**, *29*, 1605336.

[34]P. Simon, Y. Gogotsi, *Nat. Mater.* **2008,** *7*, 845.

[35]L. L. Zhang, X. S. Zhao, *Chem. Soc. Rev.* **2009**, *38*, 2520.

[36]V. Augustyn, P. Simon, B. Dunn, *Energy Environ. Sci.* **2014**, *7*, 1597.

[37]J. Chang, M. Jin, F. Yao, T. H. Kim, V. T. Le, H. Yue, F. Gunes, B. Li, A. Ghosh, S. Xie, Y. H. Lee, *Adv. Funct. Mater.* **2013**, *23*, 5074.

[38]Y. Dong, L. Xing, K. Chen, X. Wu, *Nanomaterials* **2018**, *8*, 1.

[39]X. Zang, C. Shen, E. Kao, R. Warren, R. Zhang, K. S. Teh, J. Zhong, M. Wei, B. Li, Y. Chu, M. Sanghadasa, A. Schwartzberg, L. Lin, *Adv. Mater.* **2018**, *30*, 1704754.

[40]W. He, C. Wang, H. Li, X. Deng, X. Xu, T. Zhai, *Adv. Energy Mater.* **2017**, *7*, 1700983.

[41]L. Hu, L. Xue, J. Fu, P. Xiao, T. Zhai, H. Li, *Adv. Energy Mater.* **2020**, *10*, 2001608.

[42]Rudge, J. Davey, I. Raistrick, S. Gottesfeld, J. P. Ferraris, *J. Power Sources* **1994**, *47*, 89.

[43]N.-R. Chiou, A. J. Epstein, *Adv. Mater.* **2005**, *17*, 1679.

[44]X. Li, R. Liu, C. Xu, Y. Bai, X. Zhou, Y. Wang, G. Yuan, *Adv. Funct. Mater.* **2018**, *28*, 1.

[45]T. Xu, D. Yang, S. Zhang, T. Zhao, M. Zhang, Z.-Z. Yu, *Carbon* **2021**, *171*, 201.

[46]J. B. Goodenough, K.-S. Park, *J. Am. Chem. Soc.* **2013**, *135*, 1167.

[47]K. Li, J. Zhang, D. Lin, D.-W. Wang, B. Li, W. Lv, S. Sun, Y.-B. He, F. Kang, Q.-H. Yang, L. Zhou, T.-Y. Zhang, *Nat. Commun.* **2019**, *10*, 725.

[48]Z. Guo, L. Fan, C. Zhao, A. Chen, N. Liu, Y. Zhang, N. Zhang, *Adv. Mater.* **2022**, *34*, 2105133.

[49]Y. Liu, J. Liu, Q. Zhang, Q. Zhu, X. Liu, Z. Wang, Z. Dai, *Adv. Funct. Mater.* **2022**, *32*,

2106854.

[50]D.-H. Guan, X.-X. Wang, F. Li, L.-J. Zheng, M.-L. Li, H.-F. Wang, J.-J. Xu, *ACS Nano* **2022**, *16*, 12364.

[51]X.-X. Wang, D.-H. Guan, C.-L. Miao, D.-C. Kong, L.-J. Zheng, J.-J. Xu, *J. Am. Chem. Soc.* **2023**, *145*, 5718.

[52]S. D. Tilley, *Adv. Energy Mater.* **2019**, *9*, 1802877.

[53]X. Lu, M. Yu, G. Wang, Y. Tong, Y. Li, *Energy Environ. Sci.* **2014**, *7*, 2160.

[54]C. Shen, Y. Xie, M. Sanghadasa, Y. Tang, L. Lu, L. Lin, *ACS Appl. Mater. Interfaces* **2017**, *9*, 39391.

[55]G. Wang, L. Zhang, J. Zhang, *Chem. Soc. Rev.* **2012**, *41*, 797.

[56]B. Farhadi, I. Marriam, S. Yang, H. Zhang, M. Tebyetekerwa, M. Zhu, S. Ramakrishna, R. Jose, F. Zabihi, *J. Power Sources* **2019**, *422*, 196.

[57]K. L. Van Aken, M. Beidaghi, Y. Gogotsi, *Angew. Chem. Int. Ed.* **2015**, *54*, 4806.

[58]H. Li, J. Liang, H. Li, X. Zheng, Y. Tao, Z.-H. Huang, Q.-H. Yang, *J. Energy Chem.* **2019**, *31*, 95.

[59]S. Sarawutanukul, C. Tomon, S. Duangdangchote, N. Phattharasupakun, M. Sawangphruk, *Batter. Supercaps* **2020**, *3*, 541.

[60]S. Wang, S. Huang, M. Yao, Y. Zhang, Z. Niu, *Angew. Chem. Int. Ed.* **2020**, *59*, 11800.

[61]Z. Wang, H.-C. Chiu, A. Paolella, K. Zaghib, G. P. Demopoulos, *ChemSusChem* **2019**, *12*, 2220.

[62]Rahman, K. M. Aung, S. A. Khan, **2020,** *82*, 15175.

[63]Y. Ren, T. Zhu, Y. Liu, Q. Liu, Q. Yan, *Small* **2021**, *17*, 2008047.

[64]K. Zhu, G. Zhu, J. Wang, J. Zhu, G. Sun, Y. Zhang, P. Li, Y. Zhu, W. Luo, Z. Zou, W. Huang, *J. Mater. Chem. A* **2018**, *6*, 21360.

[65]G. Shao, R. Yu, X. Zhang, X. Chen, F. He, X. Zhao, N. Chen, M. Ye, X. Y. Liu, *Adv. Funct. Mater.* **2020**, *30*, 2003153.

[66]D. P. Chatterjee, A. K. Nandi, *J. Mater. Chem. A* **2021**, *9*, 15880.

[67]L. Dong, X. Ma, Y. Li, L. Zhao, W. Liu, J. Cheng, C. Xu, B. Li, Q.-H. Yang, F. Kang, *Energy Storage Mater.* **2018**, *13*, 96.

[68]H. Wang, W. Ye, Y. Yang, Y. Zhong, Y. Hu, *Nano Energy* **2021**, *85*, 105942.

[69]B. D. Boruah, B. Wen, S. Nagane, X. Zhang, S. D. Stranks, A. Boies, M. De Volder, *ACS Energy Lett.* **2020**, *5*, 3132.

[70]J. Neumann, M. Petranikova, M. Meeus, J. D. Gamarra, R. Younesi, M. Winter, S. Nowak, *Adv. Energy Mater.* **2022**, *12*, 2102917.

[71]J. Zhu, Y. Wang, Y. Huang, R. Bhushan Gopaluni, Y. Cao, M. Heere, M. J. Mühlbauer, L. Mereacre, H. Dai, X. Liu, A. Senyshyn, X. Wei, M. Knapp, H. Ehrenberg, *Nat. Commun.* **2022**, *13*, 2261.

[72]X. Yu, G. Liu, T. Wang, H. Gong, H. Qu, X. Meng, J. He, J. Ye, *Chem. – Eur. J.* **2022**, *28*, e202202104.

[73]J. Büttner, T. Berestok, S. Burger, M. Schmitt, M. Daub, H. Hillebrecht, I. Krossing, A. Fischer, *Adv. Funct. Mater.* **2022**, *32*, 2206958.

[74]R. Wang, H. Liu, Y. Zhang, K. Sun, W. Bao, *Small* **2022**, *18*, 2203014.

[75]S. Luo, S. Zhang, H. Yuan, Z. Wu, M. Li, *Mater. Today Commun.* **2023**, *34*, 105417.

[76]B. Van Thang, H. T. Tung, D. H. Phuc, T. P. Nguyen, T. Van Man, L. Q. Vinh, *Sol. Energy Mater. Sol. Cells* **2023**, *250*, 112042.

[77]L. Tan, A. Li, Y. Yang, J. Zhang, X. Niu, N. Li, L. Liu, L. Guo, Y. Zhu, *Angew. Chem. Int. Ed.* **2022**, *61*, e202206012.

[78]C. Xu, X. Zhang, L. Duan, X. Zhang, X. Li, W. Lü, *Nanoscale* **2020**, *12*, 530.

[79]B. D. Boruah, B. Wen, M. De Volder, *Nano Lett.* **2021**, *21*, 3527.

[80]K. Kato, A. B. Puthirath, A. Mojibpour, M. Miroshnikov, S. Satapathy, N. K. Thangavel, K. Mahankali, L. Dong, L. M. R. Arava, G. John, *Nano Lett.* **2021**, *21*, 907.

[81]X. Zhang, K. Su, A. G. A. Mohamed, C. Liu, Q. Sun, D. Yuan, Y. Wang, W. Xue, Y. Wang, *Energy Environ. Sci.* **2022**, *15*, 780.

[82]Y. Chen, Z. Chen, X. Zhang, J. Chen, Y. Wang, *Nanoscale* **2022**, *14*, 10903.

[83]W. Bao, R. Wang, C. Qian, M. Li, K. Sun, F. Yu, H. Liu, C. Guo, J. Li, *ACS Nano* **2022**, *16*, 17454.

[84]J. Wang, Y. Wang, C. Zhu, B. Liu, *ACS Appl. Mater. Interfaces* **2022**, *14*, 4071.

[85]D. Knozowski, P. V. W. Sasikumar, R. Dubey, M. Aebli, K. V. Kravchyk, G. Trykowski, M. V. Kovalenko, T. Graule, M. Wilamowska-Zawłocka, G. Blugan, *Appl. Mater. Today* **2022**, *27*, 101424.

[86]L. Ding, T. Huang, D. Zhang, P. Qi, L. Zhang, C. Lin, H. Luo, *Electrochimica Acta* **2022**, *423*, 140577.

[87]E. R. Ezeigwe, L. Dong, R. Manjunatha, Y. Zuo, S.-Q. Deng, M. Tan, W. Yan, J. Zhang, D. P. Wilkinson, *Nano Energy* **2022**, *95*, 106964.

[88]M. Li, X. Wang, F. Li, L. Zheng, J. Xu, J. Yu, *Adv. Mater.* **2020**, *32*, 1907098.

[89]Z. Li, M.-L. Li, X.-X. Wang, D.-H. Guan, W.-Q. Liu, J.-J. Xu, *J. Mater. Chem. A* **2020**, *8*, 14799.

[90]J. Li, K. Zhang, Y. Zhao, C. Wang, L. Wang, L. Wang, M. Liao, L. Ye, Y. Zhang, Y.

Gao, B. Wang, H. Peng, *Angew. Chem. Int. Ed.* **2022**, *61*, e202114612.

[91]Z. Cheng, H. Pan, F. Li, C. Duan, H. Liu, H. Zhong, C. Sheng, G. Hou, P. He, H. Zhou, *Nat. Commun.* **2022**, *13*, 125.

[92]P. Li, X. Li, Y. Guo, C. Li, Y. Hou, H. Cui, R. Zhang, Z. Huang, Y. Zhao, Q. Li, B. Dong, C. Zhi, *Adv. Energy Mater.* **2022**, *12*, 2103648.

[93]M. Yu, W. D. McCulloch, D. R. Beauchamp, Z. Huang, X. Ren, Y. Wu, *J. Am. Chem. Soc.* **2015**, *137*, 8332.

[94]J. Li, H. Liu, K. Sun, R. Wang, C. Qian, F. Yu, L. Zhang, W. Bao, *J. Mater. Chem. A* **2022**, *10*, 7326.

[95]C. Zhang, B. Fei, D. Yang, H. Zhan, J. Wang, J. Diao, J. Li, G. Henkelman, D. Cai, J. J. Biendicho, J. R. Morante, A. Cabot, *Adv. Funct. Mater.* **2022**, *32*, 2201322.

[96]Y.-H. Liu, J. Qu, W. Chang, C.-Y. Yang, H.-J. Liu, X.-Z. Zhai, Y. Kang, Y.-G. Guo, Z.-Z. Yu, *Energy Storage Mater.* **2022**, *50*, 334.

[97]X. Kong, Y. Kong, Y. Zheng, L. He, D. Wang, Y. Zhao, *Small* **2022**, *18*, 2205017.

[98]Y.-H. Liu, J. Qu, W. Chang, C.-Y. Yang, H.-J. Liu, X.-Z. Zhai, Y. Kang, Y.-G. Guo, Z.-Z. Yu, *Energy Storage Mater.* **2022**, *50*, 334.

[99]Y. Qu, X. He, J. Hu, L. Duan, J. Wang, S. Liao, F. Lu, *J. Power Sources* **2023**, *555*, 232374.

[100] S. Lei, Z. Liu, C. Liu, J. Li, B. Lu, S. Liang, J. Zhou, *Energy Environ. Sci.* **2022**, *15*, 4911.

[101] B. D. Boruah, M. D. Volder, *J. Mater. Chem. A* **2021**, *9*, 23199.

[102] B. Boruah Deka, A. Mathieson, S. K. Park, X. Zhang, B. Wen, L. Tan, A. Boies, M. De Volder, *Adv. Energy Mater.* **2021**, *11*, 2100115.

[103] B. D. Boruah, B. Wen, M. De Volder, *ACS Nano* **2021**, *15*, 16616.

[104] P. Chen, T.-T. Li, Y.-B. Yang, G.-R. Li, X.-P. Gao, *Nat. Commun.* **2022**, *13*, 64.

[105] R. Khezri, S. Rezaei Motlagh, M. Etesami, A. A. Mohamad, F. Mahlendorf, A. Somwangthanaroj, S. Kheawhom, *Chem. Eng. J.* **2022**, *449*, 137796.

[106] M. Xu, H. Dou, Z. Zhang, Y. Zheng, B. Ren, Q. Ma, G. Wen, D. Luo, A. Yu, L. Zhang, X. Wang, Z. Chen, *Angew. Chem. Int. Ed.* **2022**, *61*, e202117703.

[107] Y. Zhang, J. Wang, M. Alfred, P. Lv, F. Huang, Y. Cai, H. Qiao, Q. Wei, *Energy Storage Mater.* **2022**, *51*, 181.

[108] T. S. Andrade, V. Dracopoulos, M. C. Pereira, P. Lianos, *J. Electroanal. Chem.* **2020**, *878*, 114709.

[109] T. S. Andrade, M. C. Pereira, P. Lianos, *J. Electroanal. Chem.* **2020**, *878*, 114559.

[110] D. Zhu, Q. Zhao, G. Fan, S. Zhao, L. Wang, F. Li, J. Chen, *Angew. Chem. Int. Ed.* **2019**, *131*, 12590.

[111] D. Du, S. Zhao, Z. Zhu, F. Li, J. Chen, *Angew. Chem. Int. Ed.* **2020**, *59*, 18140.

[112] Y. Jiang, Z. Liu, Y. Lv, A. Tang, L. Dai, L. Wang, Z. He, *Chem. Eng. J.* **2022**, *443*, 136341.

[113] L. Zhang, R. Feng, W. Wang, G. Yu, *Nat. Rev. Chem.* **2022**, *6*, 524.

[114] S. Liao, X. Zong, B. Seger, T. Pedersen, T. Yao, C. Ding, J. Shi, J. Chen, C. Li, *Nat. Commun.* **2016**, *7*, 11474.

[115] K. Wedege, J. Azevedo, A. Khataee, A. Bentien, A. Mendes, *Angew. Chem. Int. Ed.* **2016**, *55*, 7142.

[116] W. Li, H.-C. Fu, Y. Zhao, J.-H. He, S. Jin, *Chem.* **2018**, *4*, 2644.

[117] W. Li, E. Kerr, M.-A. Goulet, H.-C. Fu, Y. Zhao, Y. Yang, A. Veyssal, J.-H. He, R. G. Gordon, M. J. Aziz, S. Jin, *Adv. Energy Mater.* **2019**, *9*, 1900918.

[118] J. Peng, W. Zhang, Q. Liu, J. Wang, S. Chou, H. Liu, S. Dou, *Adv. Mater.* **2022**, *34*, 2108384.

[119] J. Han, S. Lee, C. Youn, J. Lee, Y. Kim, T. Choi, *Electrochimica Acta* **2020**, *332*, 135443.

[120] Ahmed, S. Sharma, B. Adak, M. M. Hossain, A. M. LaChance, S. Mukhopadhyay, L. Sun, *InfoMat* **2022**, *4*, e12295.

[121] R. Zhao, Z. Gu, P. Li, Y. Zhang, Y. Song, *Adv. Mater. Technol.* **2022**, *7*, 2101124.

[122] L. Wei, Y. Su, Y. Ma, Y. Gu, Y. Qin, X. Wu, Y. He, X. Li, Y. Peng, Z. Deng, *Chem. Eng. J.* **2022**, *448*, 137591.

[123] F. Zhang, W. Li, Z. Xu, M. Ye, H. Xu, W. Guo, X. Liu, *Nano Energy* **2018**, *46*, 168.

[124] R. Liu, M. Takakuwa, A. Li, D. Inoue, D. Hashizume, K. Yu, S. Umezu, K. Fukuda, T. Someya, *Adv. Energy Mater.* **2020**, *10*, 2000523.

[125] J. Bi, J. Zhang, P. Giannakou, T. Wickramanayake, X. Yao, M. Wang, X. Liu, M. Shkunov, W. Zhang, Y. Zhao, *Energy Storage Mater.* **2022**, *51*, 239.

[126] J.-G. Kim, H. Yu, J. Y. Jung, M. J. Kim, D.-Y. Jeon, H. S. Jeong, N. D. Kim, *Adv. Funct. Mater.* **2022**, *32*, 2113057.

[127] R. Wu, L. Ma, X. Y. Liu, *Adv. Sci.* **2022**, *9*, 2103981.

[128] L. Li, Y.-T. Chen, Y.-C. Hsiao, Y.-C. Lai, *Nano Energy* **2022**, *94*, 106944.

[129] Y. Fu, H. Wu, S. Ye, X. Cai, X. Yu, S. Hou, H. Kafafy, D. Zou, *Energy Environ. Sci.* **2013**, *6*, 805.

[130] M. Peng, K. Yan, H. Hu, D. Shen, W. Song, D. Zou, *J. Mater. Chem. C* **2015**, *3*,

2157.

[131] X. Chen, H. Sun, Z. Yang, G. Guan, Z. Zhang, L. Qiu, H. Peng, *J Mater. Chem. A* **2014**, *2*, 1897.

[132] Z. Zhang, X. Chen, P. Chen, Guan, L. Qiu, H. Lin, Z. Yang, W. Bai, Y. Luo, H. Peng, *Adv. Mater.* **2014**, *26*, 466.

[133] Z. Chai, N. Zhang, P. Sun, Y. Huang, C. Zhao, H. J. Fan, X. Fan, W. Mai, *ACS Nano* **2016**, *10*, 9201.

[134] J. Liang, G. Zhu, C. Wang, Y. Wang, H. Zhu, Y. Hu, H. Lv, R. Chen, L. Ma, T. Chen, Z. Jin, J. Liu, *Adv. Energy Mater.* **2017**, *7*, 1601208.

[135] Z. Zhang, Y. Li, R. Xu, W. Zhou, Y. Li, S. T. Oyakhire, Y. Wu, J. Xu, H. Wang, Z. Yu, D. T. Boyle, W. Huang, Y. Ye, H. Chen, J. Wan, Z. Bao, W. Chiu, Y. Cui, *Science* **2022**, *375*, 66.

[136] J. Janek, W. G. Zeier, *Nat. Energy* **2023**, *8*, 230.

[137] Y. Liu, J. Yi, Y. Qiao, D. Wang, P. He, Q. Li, S. Wu, H. Zhou, *Energy Storage Mater.* **2018**, *11*, 170.

[138] Z. Fang, Y. Zhang, X. Hu, X. Fu, L. Dai, D. Yu, *Angew. Chem. Int. Ed.* **2019**, *58*, 9248.

[139] H. Song, S. Wang, X. Song, J. Wang, K. Jiang, S. Huang, M. Han, J. Xu, P. He, K. Chen, H. Zhou, *Energy Environ. Sci.* **2020**, *13*, 1205.

[140] J. Shan, C. Ye, Y. Jiang, M. Jaroniec, Y. Zheng, S.-Z. Qiao, *Sci. Adv.* **2022**, *8*, eabo0762.

[141] Z. Liang, J. Shen, X. Xu, F. Li, J. Liu, B. Yuan, Y. Yu, M. Zhu, *Adv. Mater.* **2022**, *34*, 2200102.

[142] S. Rasal, S. Yadav, A. Yadav, A. A. Kashale, S. T. Manjunatha, A. Altaee, J.-Y. Chang, *ACS Appl. Nano Mater.* **2021**, *4*, 6515.

[143] X. Zhou, F. Yan, A. Lyubartsev, B. Shen, J. Zhai, J. C. Conesa, N. Hedin, *Adv. Sci.* **2022**, *9*, 2105792.

[144] X. Xie, N. Zhang, *Adv. Funct. Mater.* **2020**, *30*, 2002528.

[145] N. Yang, S. Yu, J. V. Macpherson, Y. Einaga, H. Zhao, G. Zhao, G. M. Swain, X. Jiang, *Chem. Soc. Rev.* **2019**, *48*, 157.

[146] Z. Jian, N. Yang, M. Vogel, Z. Zhou, G. Zhao, P. Kienitz, A. Schulte, H. Schönherr, T. Jiao, W. Zhang, X. Jiang, *Small Methods* **2020**, *4*, 2000257.

[147] M. Y. Masoomi, A. Morsali, A. Dhakshinamoorthy, H. Garcia, *Angew. Chem. Int. Ed.* **2019**, *131*, 15330.

[148] J. Li, X. Jing, Q. Li, S. Li, X. Gao, X. Feng, B. Wang, *Chem. Soc. Rev.* **2020**, *49*, 3565.

[149] Banerjee, X. Wang, C. Fang, E. A. Wu, Y. S. Meng, *Chem. Rev.* **2020**, *120*, 6878.

[150] H. Wang, J. Cao, Y. Zhou, X. Wang, H. Huang, Y. Liu, M. Shao, Z. Kang, *Nano Res.* **2021**, *14*, 3886.

[151] Mathur, R. Kaushik, A. Halder, *Catal. Sci. Technol.* **2020**, *10*, 7352.

This review article systematically summarizes the state-of-art of photo-assisted energy storage devices, covering their working principles, types, components, and various practical applications. The challenges of these photo-assisted energy storage devices are further discussed and outlined together with their future perspectives.